



The Flanks of the Rift - Second-day Road Log from Taos of Taos Pueblo, Llano Quemado, Pilar and Return to Taos

Paul W. Bauer, Adam S. Read, Keith I. Kelson, William R. Muehlberger, and Daniel J. Koning
2004, pp. 37-76. <https://doi.org/10.56577/FFC-55.37>

in:
Geology of the Taos Region, Brister, Brian; Bauer, Paul W.; Read, Adam S.; Lueth, Virgil W.; [eds.], New Mexico Geological Society 55th Annual Fall Field Conference Guidebook, 440 p. <https://doi.org/10.56577/FFC-55>

This is one of many related papers that were included in the 2004 NMGS Fall Field Conference Guidebook.

Annual NMGS Fall Field Conference Guidebooks

Every fall since 1950, the New Mexico Geological Society (NMGS) has held an annual [Fall Field Conference](#) that explores some region of New Mexico (or surrounding states). Always well attended, these conferences provide a guidebook to participants. Besides detailed road logs, the guidebooks contain many well written, edited, and peer-reviewed geoscience papers. These books have set the national standard for geologic guidebooks and are an essential geologic reference for anyone working in or around New Mexico.

Free Downloads

NMGS has decided to make peer-reviewed papers from our Fall Field Conference guidebooks available for free download. This is in keeping with our mission of promoting interest, research, and cooperation regarding geology in New Mexico. However, guidebook sales represent a significant proportion of our operating budget. Therefore, only *research papers* are available for download. *Road logs*, *mini-papers*, and other selected content are available only in print for recent guidebooks.

Copyright Information

Publications of the New Mexico Geological Society, printed and electronic, are protected by the copyright laws of the United States. No material from the NMGS website, or printed and electronic publications, may be reprinted or redistributed without NMGS permission. Contact us for permission to reprint portions of any of our publications.

One printed copy of any materials from the NMGS website or our print and electronic publications may be made for individual use without our permission. Teachers and students may make unlimited copies for educational use. Any other use of these materials requires explicit permission.

This page is intentionally left blank to maintain order of facing pages.

THE FLANKS OF THE RIFT

SECOND-DAY ROAD LOG FROM TAOS TO TAOS PUEBLO, LLANO QUEMADO, PILAR, AND RETURN TO TAOS

PAUL W. BAUER, ADAM S. READ, KEITH I. KELSON, WILLIAM R. MUEHLBERGER,
AND DANIEL J. KONING

Assembly Point: Sagebrush Inn, Taos

Departure Time: 7:30 AM

Distance: 49.4 miles

Five stops plus two optional stops

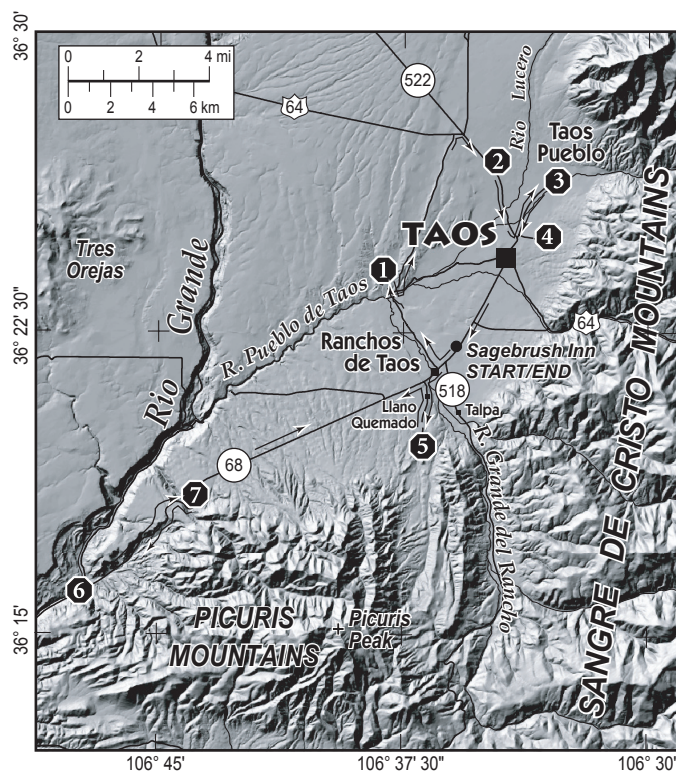
SUMMARY

Day two will focus on the tectonic development of the southern San Luis Basin, including the evolution of rift-bounding structures such as the Sangre de Cristo and Embudo fault zones. This trip will be short on driving time and generous on field time. In addition to touring part of the ancient Taos Pueblo, we have been given permission to visit several sites on Taos Pueblo tribal lands that are normally closed to the public. For that reason, *we will not include mileages for road log entries at sites on tribal lands*. Please be respectful of the hospitality the people of Taos Pueblo have extended to the New Mexico Geological Society. While at Taos Pueblo, we will discuss the hydrogeology of the Taos Valley and the earthquake history of the Sangre de Cristo fault zone. Upon leaving the pueblo, we travel westward along the northern flank of the Picuris Mountains and the Embudo fault, the best-exposed accommodation zone in the Rio Grande rift. Along the way we will discuss the structurally complex intersection between the accommodation zone and the rift master fault, examine the early rift fill sediments of the Picuris Formation and a Laramide graben, and evaluate seismic hazards along the rift boundary faults. At our last stop in the village of Pilar, we see Proterozoic rocks of the Picuris Mountains, discuss the tectonic development of the Embudo fault zone and its syntectonic sediments, and estimate slip rates and extension rates for the southern San Luis Basin.

0.0 Depart from the southwest entrance of the Sagebrush Inn. Turn right on NM-68.

The next 8.4 miles are logged in more detail in the Day 1 road log. **0.0**

0.5 On the left is the junction with NM-518 to Talpa. **Continue straight** into the Village of Ranchos de Taos. **0.5**



0.8 Turn right onto NM-240 towards Los Cordovas, Ranchitos, and the Martinez Hacienda. 0.3

3.1 Bear right, just after sharp left bend, staying on NM-240. 2.3

3.2 Crossing the Rio Pueblo de Taos. A few miles downstream of here, a knickpoint of this perennial stream is cutting Servilleta Basalt (Figs. 2.1 and 2.2). This is in contrast to the Rio Hondo to the north that is graded to the Rio Grande. **0.1**

STOPS 1-4 are on Pueblo of Taos lands, and ACCESS IS BY PERMISSION ONLY. Under no circumstances should anyone enter tribal lands without permission from the tribal government.



FIGURE 2.1. View north across the modern Rio Pueblo de Taos floodplain showing river-cut exposure of the Servilleta Basalt and overlying Quaternary fan deposits. The scalloped upper basalt contact probably represents cross sections of individual basalt flows. Nearby exposures of pillow basalt and lacustrine clay atop basalt indicate that there were ponds and/or streams here in Pliocene time.

STOP 1a. An overview of the southern San Luis

[26] **Basin. Gather for discussion.**

(Mileages for stops on the Pueblo are not included in this log.)

Geography and general geology:

This overview provides us with a good introduction to the geology of the southern San Luis Basin (Fig. 2.3) We are standing on the distal extent of a very large, complex, Pliocene to Pleistocene, alluvial fan (Fig. 2.4) that prograded into the San Luis Basin from several major drainages in the Sangre de Cristo Mountains to the north. From here we can look up the fan to the northeast into the Hondo, Seco, and Lucero canyons. Just to the south of here is the Rio Pueblo de Taos, a major perennial tributary to the Rio Grande. Although the Rio Pueblo de Taos has cut only a modest canyon in this reach, a few miles downstream it plunges precipitously into a deeply incised canyon cut through the Servilleta Basalt (Figure 2.1). Past the Rio Pueblo de Taos to the south, a series of coalesced Pleistocene alluvial fans have formed across the Embudo fault accommodation zone from drainages in the Picuris Mountains. The Picuris Mountains are a Proterozoic-cored uplift dominated by a large, overturned syncline of the Ortega Formation quartzite and younger schists, phyllites, and quartzites of the Rinconada, Pilar, and Piedra Lumbre Formations.

To the east, the Sangre de Cristo Mountains define the tectonically active, rift-flanking uplift across the Sangre de Cristo fault zone. To the north of the Rio Pueblo de Taos drainage, the range is composed of Paleoproterozoic metamorphic and metaplutonic rocks intruded by Oligocene to Miocene igneous rocks of the Questa/Latir volcanic field. South of the Rio Pueblo de Taos, the lower and more subdued topography of the Sangre de Cristo Mountains is due to relatively flat-lying sedimentary strata of Pennsylvanian age. Separating the Picuris and Sangre de Cristo Mountains are a series of north-trending valleys that mark the northern extent of the 8-km-wide Picuris-Pecos fault system. On the distant skyline to the west are the predominantly Proterozoic rocks of the Tusas Mountains of the Brazos uplift.

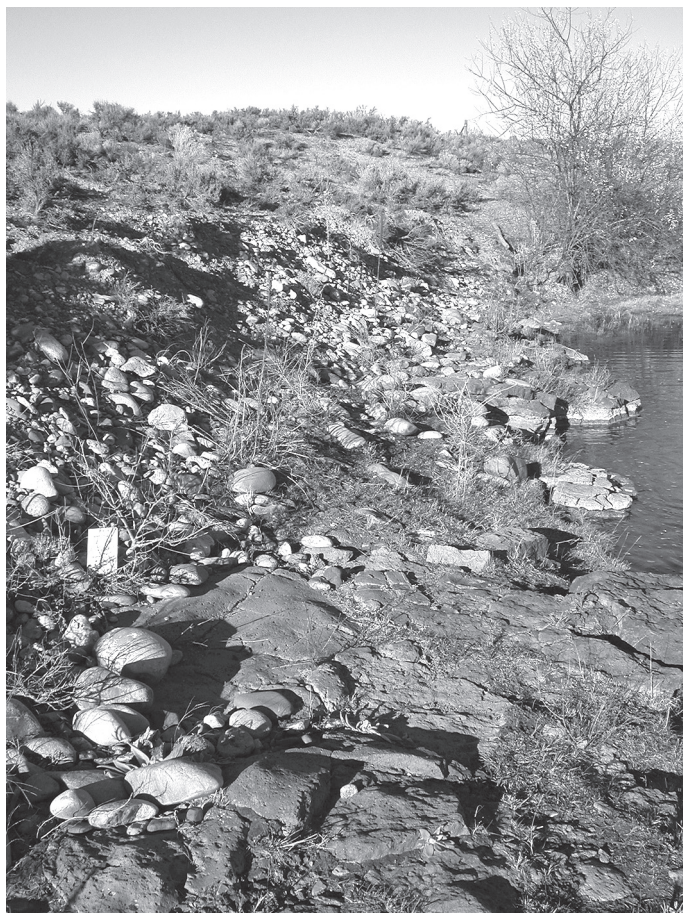


FIGURE 2.2. Cobble gravel transported by the Rio Pueblo de Taos composed of sedimentary, crystalline, and metamorphic rocks from the Taos Range. The majority of clasts are Precambrian crystalline and metamorphic rocks, although these rocks make up only a small part of the Rio Pueblo de Taos drainage area. Along the Los Cordovas stretch of the Rio Pueblo de Taos, these gravels rest on a basalt strath.

We are standing on the southeast corner of an interesting fault swarm called Los Cordovas fault zone (see Fig. 1.2 and Plate 6). The major, south-flowing drainages west of here are fault valleys in which the Servilleta Basalt has been down-dropped to the west along high-angle normal faults. Many of the drainages in this area, including the Arroyo Seco valley just to the east, have markedly asymmetrical profiles suggestive of active east-tilting of this part of the rift basin. One theory holds that the Los Cordovas faults are domino-style block rotations related to the overall east-tilting of the basin. Another states that Los Cordovas faults are young, surficial expressions of the projection of the Picuris-Pecos fault system beneath us in the basin basement.

STOP 1b. Los Cordovas fault zone.

[27] **Walk to fault scarp overlook.**

(Mileages for stops on the Pueblo are not included in this log.)

The arroyo exposes the Blueberry Hill deposit and a Los Cordovas fault. Look north of the “yellow hill” along the Los Cordovas fault escarpment (Fig. 2.5 and Fig. 2.6). The escarpment is composed of Servilleta Basalt overlain by QTbh (Blueberry

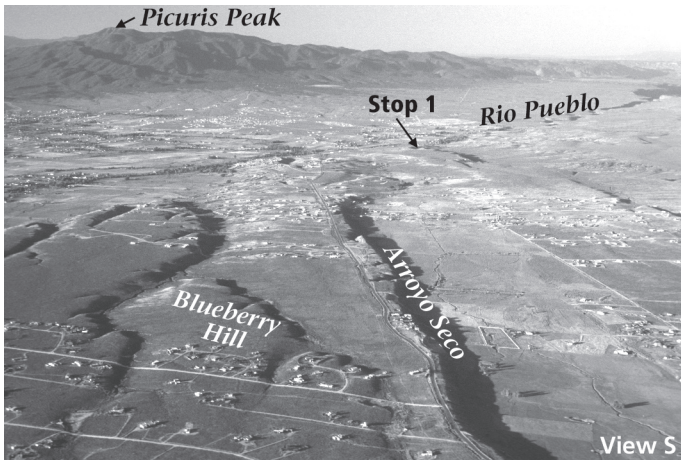


FIGURE 2.3. Aerial view south of the south-central San Luis Basin from over Blueberry Hill. Arroyo Seco and parallel, south-flowing drainages to the west join the perennial Rio Pueblo de Taos near STOP 1. A short distance west of STOP 1, the Rio Pueblo forms a basalt-rimmed canyon that deepens to join the Rio Grande in the upper right corner of the photo.

Hill basin fill deposits) and Qf1 alluvial fan gravels. The yellowish hill in the middle distance is an erosional remnant of hanging wall QTbh, and its thickness of 24 m (80 ft) yields a minimum throw for this strand of the fault system. This valley is the easternmost of several such south-flowing valleys that owe their existence to a principle strand of the generally west-down Los Cordovas fault zone.

Los Cordovas faults:

Previous workers described a 5-8 km wide zone of north-striking faults (Figs. 2.7 and 2.8) in the Taos Plateau (Lambert, 1966; Machette and Personius, 1984) that were named Los Cordovas faults for the nearby village of Los Cordovas. Prior to the recent quadrangle mapping, the only detailed geologic mapping of the

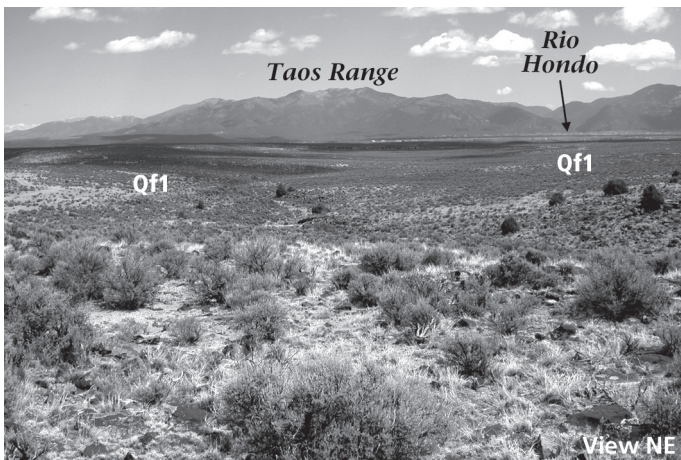


FIGURE 2.4. View looking northeast up the Qf1 alluvial-fan surface and arroyos formed on Qf1 deposits. The Qf1 surface slopes westward from the mouths of the Rio Hondo and Rio Lucero canyons in the Taos Range. The southwestern edge of the Qf1 deposits grades to (or interfingers with) deposits laid down by the south-flowing ancestral Rio Grande prior to incision into Servilleta Basalt.

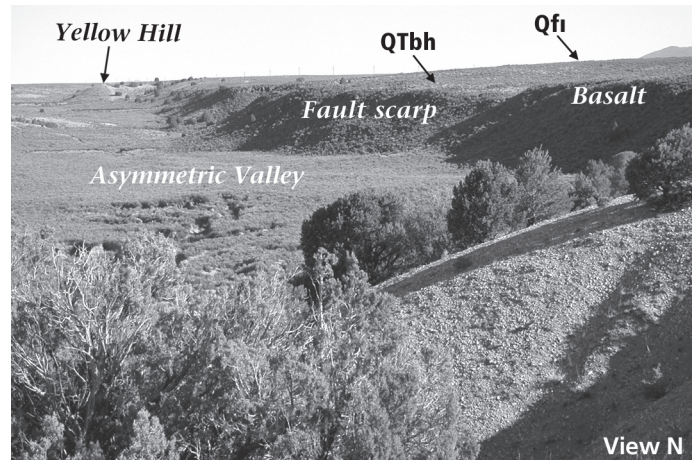


FIGURE 2.5. View north of Los Cordovas fault scarp from the overlook at STOP 1B. The footwall of the steeply west-dipping fault consists of Servilleta Basalt overlain by Blueberry Hill deposits (QTbh) and Qf1 alluvial deposits. Although the hanging wall deposits have mostly been stripped by the drainage, the Blueberry Hill deposits exposed at Yellow Hill indicate that there is at least 24 m (80 ft) of throw on this strand of the fault.

faults was by Kelson (1986), who mapped their southernmost extent along the Rio Pueblo de Taos. Where separation is greatest, the faults juxtapose piedmont-slope alluvium down to the west against older Servilleta Basalt. Machette and Personius (1984) stated that the fault offset is greater than the 15-30 m high erosional scarps that now define the surface expression, and that faulting may be as old as early Pleistocene, but could be as young as middle(?) Pleistocene. Profiles of stream terraces along the Rio Pueblo de Taos suggest that the faults displace the early(?) to middle Pleistocene piedmont surface, but not the middle Pleistocene Qt₂ terrace (Kelson, 1986; Machette et al., 1998).

Los Cordovas faults are located above the deepest part of the Taos graben. The faults are rather uniformly spaced, barely diverge from a north-south trend, are nearly all west-down, and

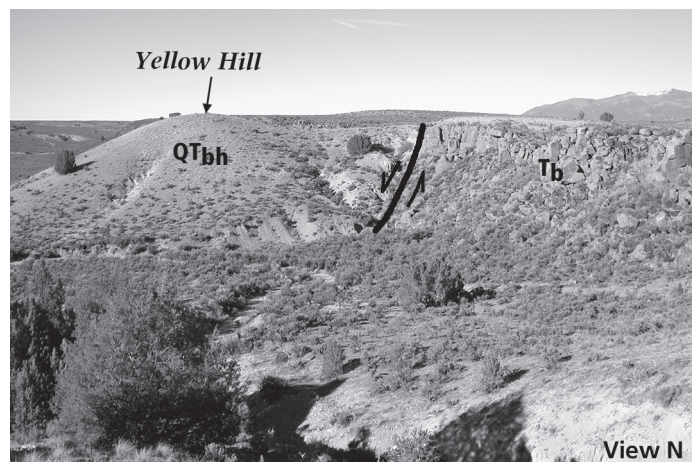


FIGURE 2.6. Close-up of Yellow Hill showing the trace of Los Cordovas fault and the juxtaposition of Blueberry Hill deposits (QTbh) against Servilleta Basalt (Tb). Slickenlines on faulted basalt at Yellow Hill dip steeply west.

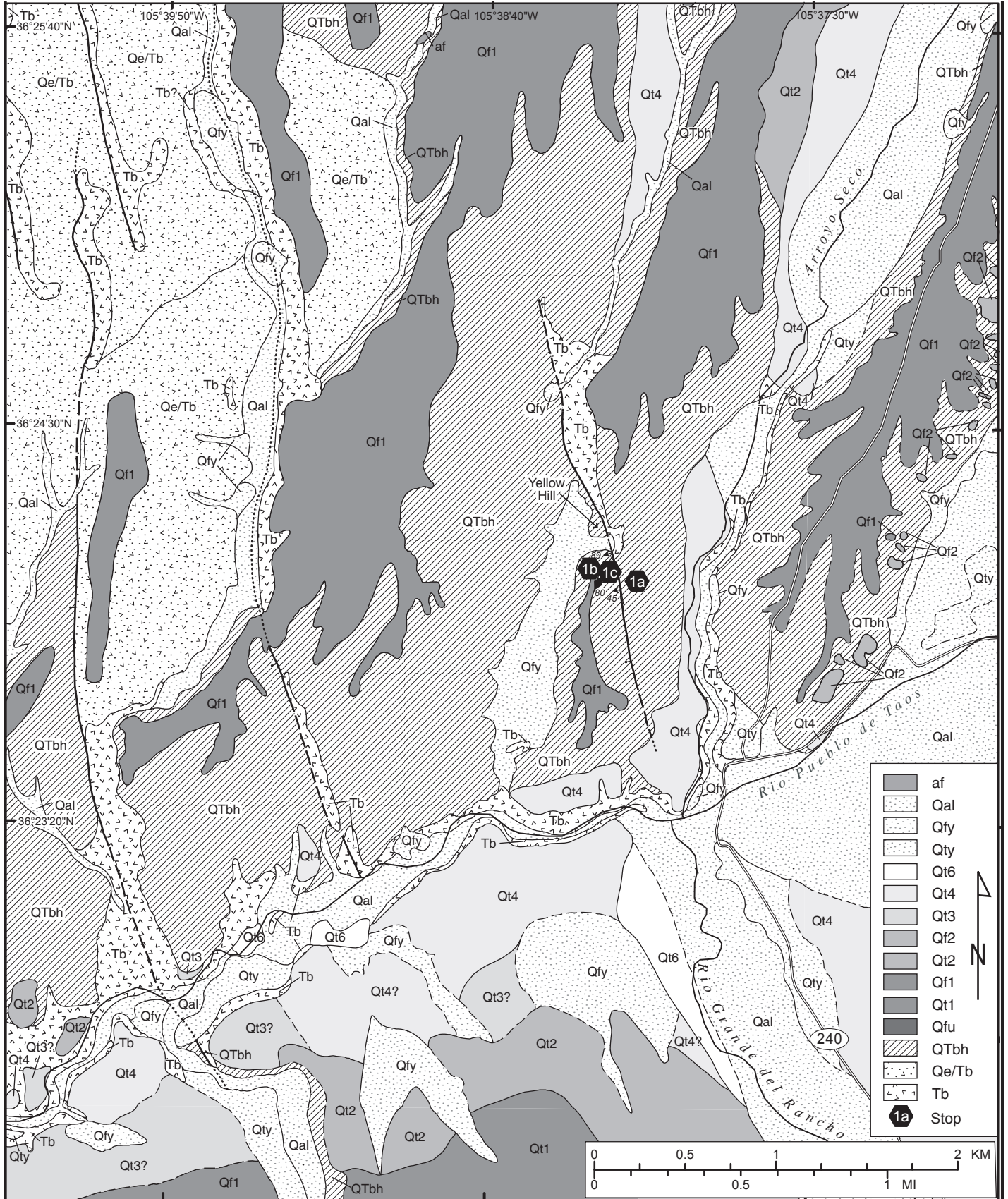


FIGURE 2.7. Geologic map of the Los Cordovas area, west of Blueberry Hill, and the site of Stops 1a, b, and c. Modified from Kelson and Bauer (2003), Bauer and Kelson, (2001), Bauer et al. (1999), and Bauer and Kelson (1997).

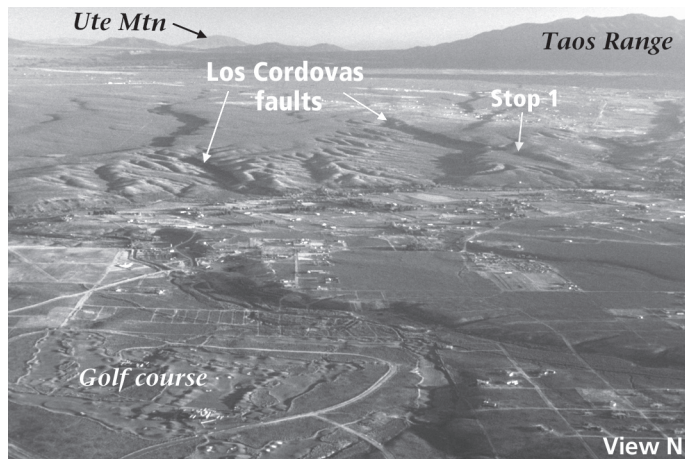


FIGURE 2.8. Aerial view north along two major exposures of Los Cordovas fault system, just west of STOP 1. Both faults are characterized by steep, foot wall bluffs against eroded, Blueberry Hill deposits of hanging wall.

appear to surface-terminate to the north and south (see Plates 2, 3, and 4). Lambert (1966) noted that they are directly on trend with both the Picuris-Pecos fault to the south, and the Sangre de Cristo fault to the north, but failed to speculate on a possible connection. We believe that the Picuris-Pecos fault system exists in the subsurface of the Taos graben (Bauer and Kelson, 2004, this volume). We do not know the locations of strands of the Picuris-Pecos fault in the subsurface beneath the Taos Plateau, but we agree with Lambert (1966) that the Los Cordovas faults could be related to these older structures. The fact that the Los Cordovas faults are short, west-down, and are located over the deepest part of the basin suggests that they could be antithetic, west-dipping faults that intersect the Taos graben at depth. On cross sections, Bauer and Kelson (2004, this volume) have chosen to speculatively show the major strands of the Picuris-

Pecos fault system as major, Laramide, rift-reactivated structures that shallow into the Pleistocene Los Cordovas faults.

Blueberry Hill deposits:

At this point, we are standing on a thin eolian mantle deposited on the Blueberry Hill deposits (unit Qtbh, Bauer et al., 2001), which contain primarily sand and pebble conglomerate beds and are moderately consolidated (Fig. 2.9). Overall, the near-surface Qtbh deposits are finer grained with distance southwestward from the Sangre de Cristo mountain front. The deposits are distinct by comparison with younger, stratigraphically higher deposits, such as the Qf1 fan deposits, because the Qtbh gravel clasts are smaller (primarily pebbles and few cobbles; Kelson, 1986). In addition, the Qtbh deposits commonly are highly oxidized and clasts are stained with black oxide coatings (probably Mn). The staining and oxidation may be related to groundwater saturation, as it commonly cross-cuts bedding. The Blueberry Hill deposits also locally include fine-grained clay beds that may have been deposited in a lacustrine environment. We interpret that the deposits represent fluvial and alluvial-fan aggradation within a broad montane piedmont, which was present prior to the development of the Rio Grande gorge. Upon incision of the Rio Grande and Rio Pueblo de Taos canyons, and capture of surface and groundwater flow, the high groundwater level probably declined.

The stratigraphic relationship between the Blueberry Hill deposits and the oldest Rio Grande gravel (unit Qt1rg, Kelson and Bauer, 2003) is unclear. The Qt1rg gravel may be inset into the Blueberry Hill deposits, or these deposits are interfingered with each other. If the Blueberry Hill deposits interfinger with the Qt1rg deposits, they represent the local mountain-front piedmont deposits that are graded to pre-incision axial gravels of the Rio Grande.

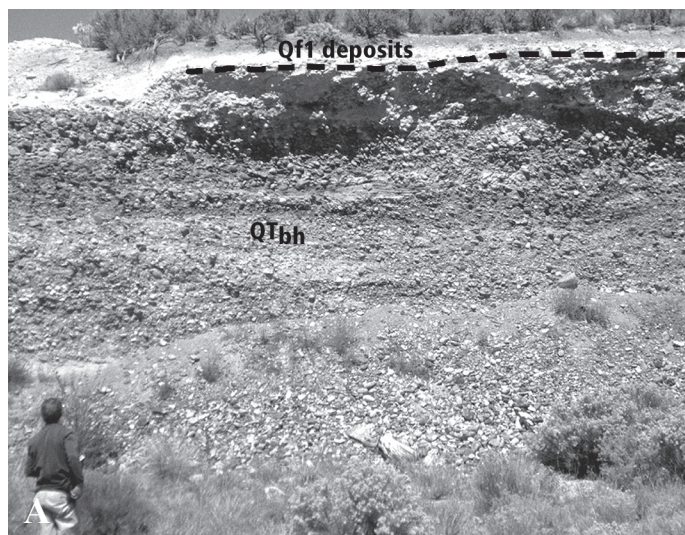


FIGURE 2.9. Photograph of Plio-Pleistocene Blueberry Hill deposits (Qtbh) exposed in abandoned gravel quarry south of Rio Pueblo de Taos. Exposure shows bedding (A), imbrication (B), and staining that are characteristic of Qtbh, although south of Rio Pueblo de Taos, unit Qtbh contains an unusually high percentage of sedimentary clasts (>50%) relative to metamorphic and crystalline clasts lithologies. Uppermost 1 m of quarry exposure is fine-grained deposits associated with the Qf1 alluvial-fan surface, and contains a well-developed carbonate soil profile. Pencil for scale in B.

STOP 1c. Los Cordovas Faults in Outcrop**[28] Walk down into arroyo and up to fault exposure.***(Mileages for stops on the Pueblo are not included in this log.)*

The walls of the arroyo west of the fault provide 4-m-high exposures (Fig. 2.10) of the upper Blueberry Hill deposits (Kelson and Bauer, 2003), which consist of bedded pebble gravel and sand, oxidized to yellowish orange. Local sand beds are up to about 30 cm thick. A several-meter-thick, yellowish silty clay is exposed on the northern arroyo wall. A sample analyzed by G. Austin at the NMBGMR Clay Lab was found to be very fine grained, sticky but not bentonitic, well-crystalline, very clean, and composed mostly of illite and smectite with minor quartz. This clay is interpreted to be lake sediment derived from highly altered volcanic rocks.

Fault geometry and kinematics:

The easternmost exposed strand of the Los Cordovas fault zone can be seen in the arroyo (Fig. 2.11). The hanging wall of this west-dipping fault consists of the bedded Blueberry Hill gravel deposits, overlain by younger hillslope colluvium. Deposits exposed in the footwall consist of Servilleta Basalt on the floor of the arroyo, which is overlain by a deep reddish silty clay. The fine-grained reddish clay deposit is similar to the nearby yellow clay (see above), in that it is also very fine grained, sticky but not bentonitic, well-crystalline, very clean, and composed mostly of illite and smectite with minor quartz. The clay is also



FIGURE 2.10. Photograph of 4-m-thick yellow clay exposed on north wall of unnamed arroyo at STOP 1B. Laboratory analysis has shown that the material is very fine grained, sticky but not bentonitic, well-crystalline, very clean with minor quartz, and composed mainly of illite and smectite, and probably represents a lake deposit (G. Austin, personal commun., 2001).

interpreted to be lake sediment, thought to be derived from highly altered volcanic rocks that were deposited in a short-lived lake (or playa) within the broad, pre-gorge Rio Grande valley. In some places, pillow basalts (Fig. 2.12) also indicate that standing water was present during Servilleta Basalt volcanism. The clay is overlain by unfaulted hillslope colluvium that was shed from Blueberry Hill deposits to the east. The soil formed in this colluvium is weakly developed and suggests that the colluvium is an active Holocene deposit.

The exposed fault strand displaces the upper Blueberry Hill gravel on the west against the fine-grained clay on the east, but does not extend into the younger hillslope colluvium. The primary fault strand dips 45° west. Kinematic indicators on the fault plane include down-dip slickenlines as well as rotated and aligned cobbles, suggesting a west-down sense of vertical separation; an interpretation confirmed by the west-down sense of displacement of the Servilleta Basalt and the Blueberry Hill deposit. Just to the north of here, at the yellow hill, near-vertical (89° west dip) fault planes show down-dip slickenlines on the Servilleta Basalt in the footwall of this same Los Cordovas fault segment.

The age of faulting:

Lambert (1966) suggested that the Los Cordovas fault exhibited Pleistocene displacement, and Machette and Personius (1984) interpreted possible middle Pleistocene movement on the basis of displacement of surficial deposits inferred to be early Pleistocene. Kelson (1986) interpreted that the Qf1 fan surface is displaced by the Los Cordovas faults, and that the inset Qt2 terrace along Rio Pueblo de Taos is not displaced (Fig. 2.13). These relations support a middle Pleistocene age for the most-recent movement on the fault, as interpreted by Machette and Personius (1984) and Personius and Machette (1984). The arroyo exposure at this field trip stop provides no additional constraint on the age of recent faulting on this strand. The overall map pattern and location of the Los Cordovas faults (Plates 2, 3, and 4) are similar to that of the older Picuris-Pecos fault system, which also consists of a series of north-striking faults that separate long, linear blocks about 1-to-2 km wide. Bauer and Kelson (2004a, this volume) suggest that the Los Cordovas faults may represent a reactivation of the Picuris-Pecos fault system during rifting of the southern San Luis Basin in the Neogene.

**Return to vehicles and backtrack to NM-240
where we will continue north.**

3.4 Turn left onto Blueberry Hill Rd. Note the fresh burn scar from the Encebado fire of summer 2003 east of Taos Pueblo in the Sangre de Cristo Mountains at 2:00-3:00. The fire was started by a lightning strike on July 4th in Encebado Canyon, less than a mile from Taos Pueblo. Before it was contained 11 days later, it burned 5400 acres of Taos Pueblo land including many sacred sites. Over 1000 firefighters and 15 aircraft were called in to fight the blaze. The pueblo government has formulated a plan designed to prevent an Encebado-type disaster from ever happening again and is working to restore

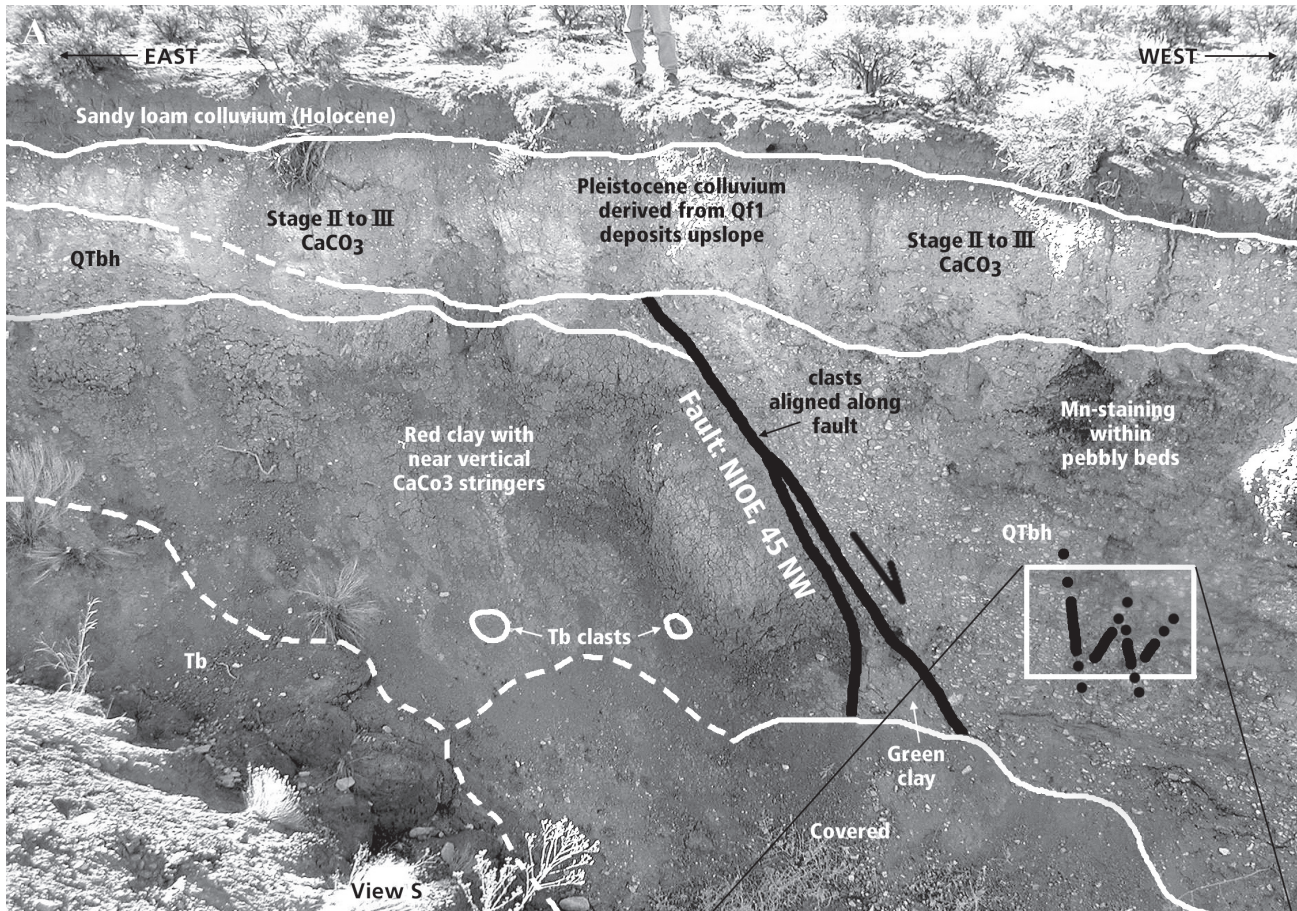


FIGURE 2.11. Photograph (A) of fault exposure in unnamed arroyo incised across the eastern strand of the Los Cordovas fault zone at STOP 1B. The eastern footwall block contains Pliocene Servilleta Basalt (Tb) overlain by a local, red lacustrine clay (composed of illite plus smectite), and Plio-Pleistocene Blueberry Hill deposits (QTbh), faulted against QTbh deposits on the hanging-wall. The red clay is highly fractured with good down-dip slickenlines on fault planes that dip 45° towards 260° azimuth. Flat cobbles are aligned along the fault plane. QTbh contains black Mn staining on bedding. The fault is overlain by undisplaced Pleistocene and Holocene colluvial deposits. Inset photograph (B) shows the details of complex, minor, horst and graben faults in hanging wall. Geologists legs for scale in top center of photo.



55th NMGS FFC 2004
Second-day Road Log

damage from the fire. Later in the summer of 2003, monsoonal rains spawned a series of destructive mudflows in the arroyos below the burn area. **0.2**

8.2 Turn right at intersection with US-64. [5] 4.8

8.4 Turn right onto NM-522 at light. This intersection was formerly known as the “Blinking Light.” [6] 0.2

8.8 We are driving on Qfy of Bauer and Kelson (2001), young alluvial deposits derived from the Rio Lucero and Arroyo Seco drainages. The subtle topographic rise at El

Prado represents the slightly older Qf2 deposits and corresponding geomorphic surface. **0.4**

9.8 The unmarked dirt road on left, just before the [29] Overland Sheepskin Company, leads to the Buffalo Pasture area of Taos Pueblo, which is the site of Stop 2. ACCESS IS BY PERMISSION ONLY. 1.0

STOP 2. The Pow Wow grounds on Taos Pueblo. [30] Gather for discussion.

(Mileages for stops on the Pueblo are not included in this log.)
At this stop we will discuss the Sangre de Cristo fault system,



FIGURE 2.12. A rare exposure of pillow structures in Servilleta Basalt exposed in the Rio Pueblo de Taos drainage southwest of STOP 1. Such structures, along with lacustrine clays, and highly oxidized “baked zones” below basalt flows indicate that standing water existed here in late Pliocene time when basalts were erupting. GPS for scale.

the Buffalo Pasture, and the hydrogeology of the area. This area is on tribal land and access is by permission only. However, much of this area can be easily viewed from nearby non-tribal lands.

Geology of the Buffalo Pasture area:

We are situated along the north end of the Taos Pueblo Buffalo Pasture (Fig 2.15), a remarkably lush and pristine wetland that is sacred to the native inhabitants. To the east, along the break in slope between the piedmont and the mountains, are a series of large fault scarps of the Sangre de Cristo fault system. The south end of the Buffalo Pasture is bordered by the alluvial valley of the Rio Pueblo de Taos. West and north of the pasture are a series of eroded Pleistocene alluvial fans that were derived from the mountain canyons to the north. Although Bauer and Kelson (2001) mapped these wetlands as a distinct geologic unit (Qm marsh deposits), they acknowledged that the original deposits are equivalent to surrounding basin fill units, but their degree of alteration and soil development require that they be sub-divided.

The Buffalo Pasture area lies on the distal part of the large alluvial fan derived from the Rio Lucero drainage to the north

(Bauer and Kelson, 2001). The fan exits southwestward from the Sangre de Cristo Mountain front, and the modern Rio Lucero channel is dramatically deflected southward, parallel to the mountain front to its confluence with the Rio Pueblo de Taos southwest of the Buffalo Pasture (Fig. 2.16). Streamflow gaging data from near the mouth of Rio Lucero show high discharges during periods of high snowmelt and summer thunderstorms, although most of this discharge percolates into near-surface deposits near the mountain front, and Rio Lucero is not much more than a shallow arroyo as far south as the Buffalo Pasture. Similarly, shallow wells north of the Buffalo Pasture display a rapid water level response to climatic events (P. Johnson, personal commun., 2004). Mapping of surficial deposits show that previous courses of the Rio Lucero had more southwesterly directions and instead merged with Arroyo Seco, which continues along the western side of Blueberry Hill (Bauer and Kelson, 2001). The present-day course of Rio Lucero, Rio Seco, and alluvial-fan deposition may be influenced by east-down faulting or tilting on inferred faults located east of Blueberry Hill. In support of this theory, recent high-resolution aeromagnetic data show a major north-striking fault below Rio Lucero, and a second fault just to the east (Grauch et al., 2004, this volume; Plate 5). Neither fault has surface expression that can be mapped.

At the Buffalo Pasture, the distal parts of the Rio Lucero fan are thin and are deposited on the relatively less permeable Blueberry Hill deposits. Shallow groundwater in the Buffalo Pasture wetlands likely is a result of large contributions from Rio Lucero and thin alluvium resting on the Blueberry Hill deposits, resulting in a locally shallow perched water table (Fig 2.17). Alternatively, shallow faults may influence the near-surface groundwater distribution, although there is no prominent geomorphic evidence of active faulting in the Buffalo Pasture area.

Temperature logging of deep BIA and BOR wells:

Marshall Reiter at NMBGMR, in cooperation with the Bureau of Indian Affairs and Glorieta Geosciences, Inc., recorded down-hole temperature logs at eight well sites in the Taos area (Fig 2.18). From these data, preliminary interpretation suggests that the hydrogeology is complex both vertically and horizontally (Reiter and Sandoval, 2004, this volume). One of the principle deductions is that a major hydrologic barrier (probably a fault) exists between two wells that are just northwest of the Buffalo Pasture. The existence of such a structure is supported by the new aeromagnetic work (Grauch et al., 2004, this volume; and Plate 5).

Town Yard fault and eastern edge of the Taos graben:

The eastern edge of the Taos graben correlates with mapped and inferred structures of the Sangre de Cristo fault zone. Gravity data as interpreted by Reynolds (1992), showed a complex eastern fault zone that generally steps down into the graben. Reynolds (1986, 1992) also performed shallow seismic reflection surveys over parts of Taos Pueblo, interpreting a complex system of buried faults along the Cañon section of the fault zone, including some small-scale horst and graben geometries. Evidence exists for a southward extension of such structures into

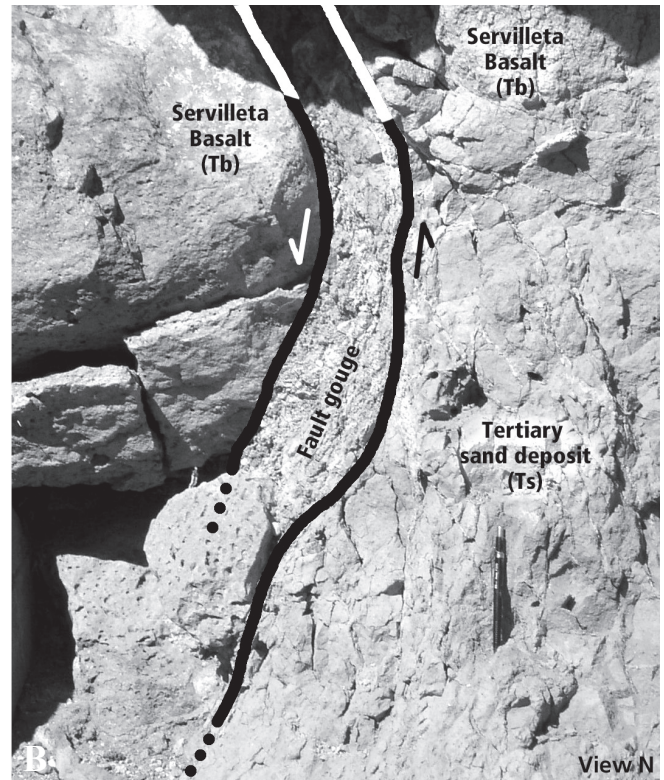


FIGURE 2.13. Photograph (A) of the western strand of Los Cordovas fault, showing west-down displacement of Servilleta Basalt (Tb) on the south side of the Rio Pueblo de Taos. The fault is overlain by undisplaced late Pleistocene to Holocene alluvial deposits that flank the Rio Pueblo de Taos. A close-up of the fault zone (B) shows a 15-cm-thick, red, clay-rich, strongly foliated shear zone along the fault plane that juxtaposes Servilleta Basalt against Tertiary sandstone. Pencil for scale.

the Miranda graben and Picuris-Pecos fault zone in the Picuris Mountains to the south. In 1996, the Town of Taos drilled an exploration water well at the Town Yard, southwest of Taos. At about 600 ft, a 70-ft-thick basalt was encountered, and at 720 ft Pennsylvanian sedimentary strata were encountered. Drilling ceased after penetrating 300 ft of the Pennsylvanian section.

Bauer and Kelson (2004a, this volume) have depicted the Town Yard fault as a zone of west-down normal faults that separate the deep Taos graben from the shallow, structurally complex Taos embayment bench. The recent high-resolution aeromagnetic data support much of this model (Grauch et al., 2004, this volume; Plate 5) as does gravity data (Fig. 2.19).

SIDEBAR 2.1—American Bison:

Although American bison (Fig. 2.14), the largest land mammal in North America, typically appear peaceful, unconcerned, even lazy, they may attack anything, often without warning or apparent reason. A bull can outrun, out turn, and traverse rougher terrain than most horses. They can run at speeds of up to 35 miles per hour, and cover long distances at a deceptively fast lumbering gallop. They have a highly developed sense of smell, good hearing, poor sight, and will charge when cornered. By the late 1800s, after a systematic program of genocide by the U.S. government, only an estimated 1500 bison remained in North America from the estimated 30-60 million that roamed the plains prior to European settlement. The Great Plains herds are thought to have been the largest mass of large mammals ever on Earth. Today, due to legal protection, establishment of preserves, and stewardship by a variety of entities, there are over 350,000 bison, mostly in privately owned herds.



FIGURE 2.14. The Pueblo of Taos keeps a herd of American bison (*Bison bison*) in the Buffalo Pasture. These magnificent animals, being naturally curious and impulsive, add a decidedly thrilling aspect of unpredictability to geologic fieldwork in their pasture.

Photo by David J. McGraw

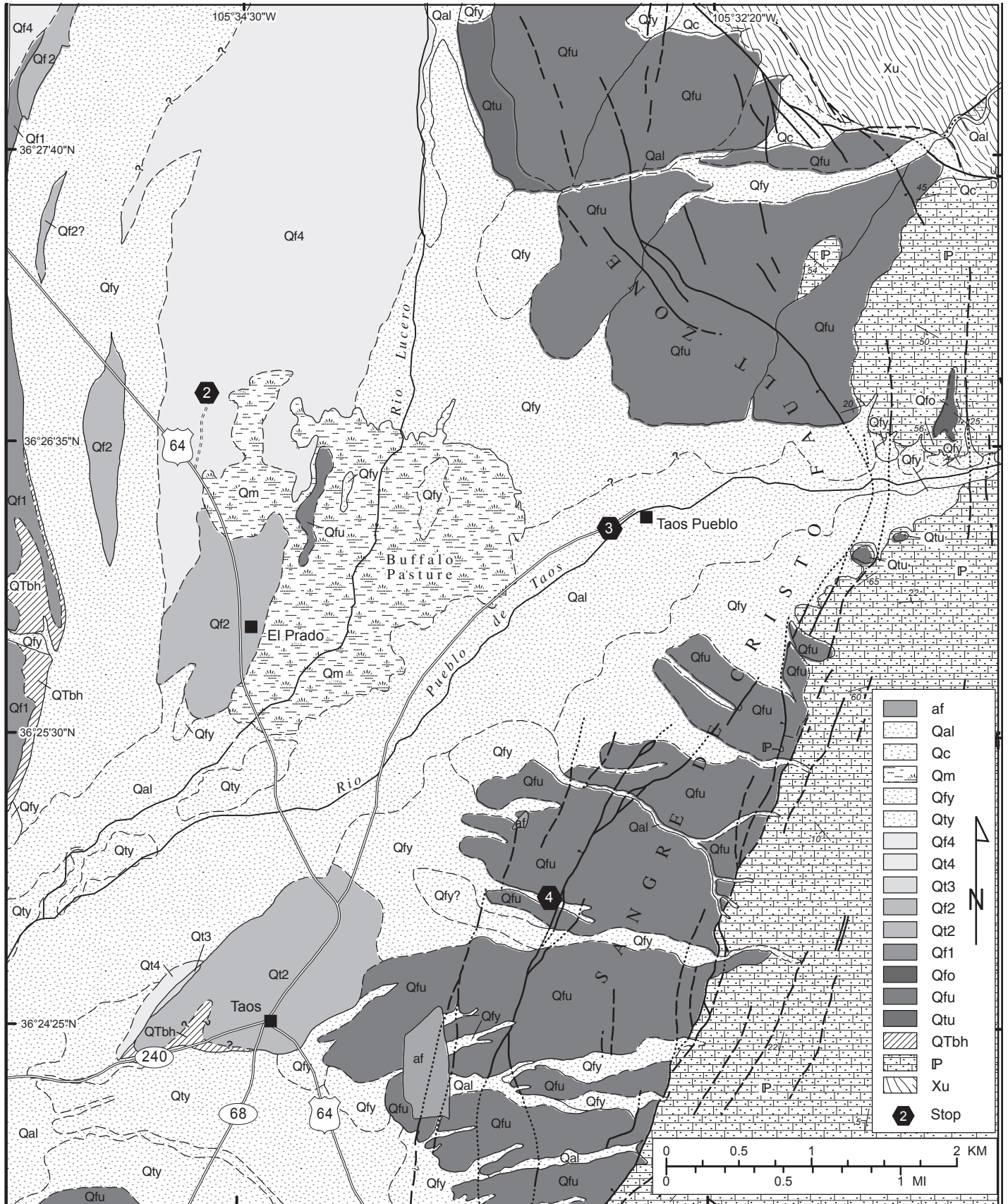


FIGURE 2.14. Geologic map of the Buffalo Pasture area, Taos quadrangle, modified from Bauer and Kelson (2001).



FIGURE 2.16. Aerial orthophotograph of the remarkable geomorphology along the Sangre de Cristo range front between the Arroyo Hondo on the north and Taos on the south. The Arroyo Seco and Rio Lucero drainages emerge westward from the mountain front, and abruptly swing southward parallel to the mountain front. We attribute this curious behavior to active tectonics, wherein this part of the San Luis Basin is rotating downward along the Sangre de Cristo fault zone. According to an interpretation of detailed aeromagnetic data, the Rio Lucero appears to be underlain by a major north-striking fault (Grauch et al., 2004 this volume; Plate 5) that has no surface expression (Bauer and Kelson, 2001).

Sangre de Cristo fault system:

The Sangre de Cristo fault is a west-dipping normal fault that forms the border between the Sangre de Cristo Mountains on the east and the San Luis Basin on the west. The southern Sangre de Cristo fault within Colorado and New Mexico is divided into five primary sections and numerous subsections based on fault-trace complexity and mountain-front and fault-scarp morphologic data (Menges, 1988; Machette et al., 1998). From north to south, these are the San Pedro Mesa, Urraca, Questa, Hondo, and Cañon sections (Machette et al., 1998). The northern three of these sections (i.e., the San Pedro Mesa, Urraca, and Questa sections) strike generally north and extend from Costilla Creek in southern Colorado to San Cristobal Creek about 25 km north of Taos.

The boundary between the Questa and Hondo sections is at a large bedrock salient of the Sangre de Cristo Mountains. In contrast to the northern sections, the Hondo section strikes about N30°W, and extends to the Rio Pueblo de Taos. The 14-km-long Cañon section strikes about N20°E, and extends from Rio Pueblo de Taos to Rio Grande del Rancho. Together, the Hondo and Cañon sections of the southern Sangre de Cristo fault border a 30-km-long, 10-km-wide, crescent-shaped re-entrant in the Sangre de Cristo range block, referred to informally as the Taos embayment.

The southern Sangre de Cristo fault shows prominent geomorphic evidence of late Quaternary surface rupture, including scarps across alluvial fans of various ages (Fig. 2.20), air-photo lineaments, springs, and alignments of vegetation. Machette and Personius (1984) and Personius and Machette (1984) profiled several scarps along the Cañon section, and suggested a Holocene age for the most-recent movement. Kelson (1986) mapped late Quaternary deposits and some fault strands along this section, and showed faulted late Pleistocene alluvial-fan deposits. Menges (1990) conducted detailed morphometric analyses of the range front and fault scarps, and suggests the possibility of early Holocene to latest Pleistocene movement along the Cañon section. Recent geologic mapping along the fault and GPS profiles of the scarp support these previous age estimates (Fig. 2.21 and Plate 6). Based on scarp morphology data, Menges (1988, 1990) estimated a recurrence interval of about 10 to 50 k.y., and Quaternary slip rates ranging from 0.03 to 0.26 mm/yr.

The Cañon section is a complex system of branching faults that is as much as 2 km wide. With the exception of the Rio Fernando area, fault scarps in Quaternary deposits are mostly confined to the mountain front, where Quaternary deposits are in fault contact with Pennsylvanian rocks. Individual fault planes typically dip steeply west to northwest, with slickenlines plunging moderately to steeply westward. The transition from strike-slip to dip-slip is gradational, with a prevalence of oblique-slip (plus some strike-slip) faults in the bedrock just southeast of Talpa. In Pennsylvanian rocks near the Rio Grande del Rancho, faults dip between 60-80° northwest with moderately west-plunging slickenlines. North of the Rio Fernando, faults dip between 70-89° westward with generally downdip slickenlines. In general, field measurements of Sangre de Cristo fault plane dips are consistently steeper than estimates based on geophysics

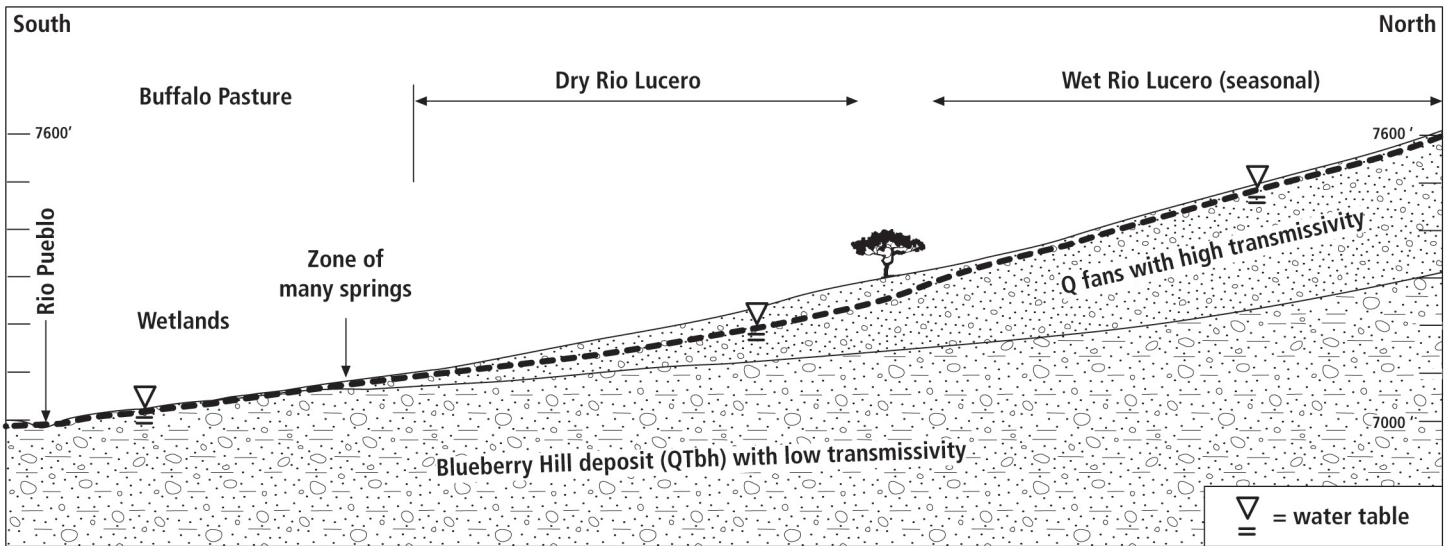


FIGURE 2.17. Schematic north-south cross section showing the hydrogeology of the Buffalo Pasture area, based on the geologic map of Bauer and Kelson (2001). In this interpretation, shallow groundwater derived from the Rio Lucero is stored in young fan deposits, and perched on the relatively impermeable Blueberry Hill deposit (QTbh). The water emerges as springs and stream flow along the northern edge of the Buffalo Pasture where the younger surficial deposits thin southward.

in the northern San Luis Basin of 40-60° by Tandon (1992) and 60° by Kluth and Schaftenaar (1994).

Despite the proximity of late Quaternary fault scarps along the Sangre de Cristo fault (Fig. 2.20 and Fig 2.22), there is no evidence of past earthquake-related damage to the 900-year-old adobe walls of the old pueblo. Paleo-earthquake magnitudes may have been as large as M 7, which probably would have resulted in damage to such unreinforced structures. However, because the recurrence interval for large earthquakes on these faults is probably longer than 10,000 years, the absence of



FIGURE 2.18. Photograph of the August 2001 drilling of the 2039-ft-deep BOR-6 production well 4 km northwest of STOP 2. This was one of six deep wells that were drilled around 2001-2 in order to provide hydrogeologic and hydrologic data to support the water rights settlement for the Taos valley. Surprisingly, the well encountered Servilleta Basalt at over 1000 ft depth, suggesting that either Pliocene basalt flows filled a deep valley, or the basalt is downfaulted.

damage in the relatively short historical time period is not surprising (see paper by Kelson et. al., 2004b, this volume).

Return to vehicles.

- 11.0 Crossing over the Rio Lucero. We are driving through the southern tip of the Buffalo Pasture wetlands. 1.2
- 11.1 On left is Hail Creek Rd, an entrance to Taos Pueblo that takes visitors to the Taos Mountain Casino. 0.1
- 11.3 Crossing over the Rio Pueblo de Taos and its broad alluvial valley. 0.2



FIGURE 2.19. This area was the focus of a detailed gravity survey in 2001 by the New Mexico Bureau of Geology and Mineral Resources. The survey consisted of 21 separate traverses with 50 m and 100 m station spacing, for a total of 66 km of survey lines.

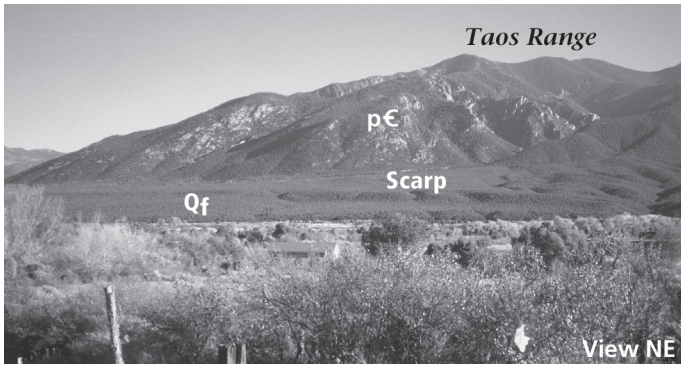


FIGURE 2.20. View northeast of the faulted range front of the Taos Range northeast of the old Pueblo of Taos. The large fault scarp offsetting a Quaternary alluvial fan is one segment of a highly segmented Sangre de Cristo fault system.

- 11.6 Stoplight at Camino de la Placita. Continue ahead, climbing onto the Pleistocene Qt2 terrace, upon which the original community of Taos was built. 0.3
- 11.8 Turn left just past gas station at main entrance into [31] Taos Pueblo. As we drive northeast towards the pueblo, the road descends from Qt2 to a younger terrace Qty to the modern alluvium of the Rio Pueblo de Taos (Qal). 0.2
- 11.9 Cattle guard and fence. 0.1
- 12.4 Bridge over the Rio Pueblo de Taos. 0.5
- 12.8 Taos Mountain Casino on left. 0.4
- 13.0 Fault scarp displacing an alluvial fan is visible straight ahead 0.2
- 13.2 Good view of the lush Buffalo Pasture to the left. 0.2
- 13.9 Arrive at Taos Pueblo visitors parking area. The old [32] pueblo village is built on the Qal floodplain of the Rio Pueblo de Taos. 0.7

STOP 3. Pueblo of Taos.
Designated a World Heritage Site in 1992.

(Mileages for stops on the Pueblo are not included in this log.) At this stop we will tour the old Pueblo area (Fig. 2.23). The Pueblo is usually open to visitors 8:30 am to 4:30 pm daily but may be closed for ceremonies without notice. Fees and other restrictions apply to photography, but guided tours are available.

Taos Pueblo history:

Taos Pueblo, probably built between 1300 and 1450 A.D., is apparently the oldest continuously inhabited permanent settlement in the United States. The adobe structure was perhaps built or substantially enlarged after abandonment of the Pot Creek Pueblo to the south (see sidebar in the Day 3 log) in about

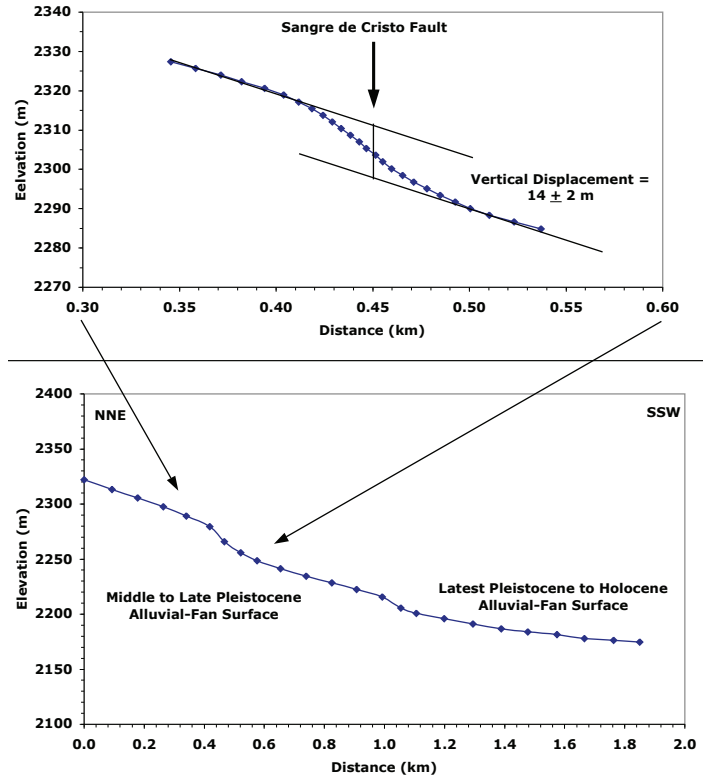


FIGURE 2.21. Topographic profiles across the primary Sangre de Cristo fault scarp developed on Pleistocene alluvial-fan deposits flanking the northern margin of Rio Pueblo de Taos, north of Taos Pueblo. The net vertical displacement of the fan surface (14 ± 2 m) is based on projection across the fault zone as shown, and likely represents multiple late Quaternary surface-rupturing earthquakes ($M > 6.5$). The lower scarp on the lower topographic profile shows the inset relationship between latest Pleistocene to Holocene fan deposits (on the south), and middle to late Pleistocene alluvial-fan deposits on the north. Data from upper profile derived from hand-level measurements; data from lower profile derived from detailed survey using differential Global Positioning System methods.

1350 A.D. when the former inhabitants, according to some anthropologists, moved to both Taos and Picuris pueblos. The two structures called *Hlauuma* (north house) and *Hlaukwima* (south house) are said to be of similar age. The native language is Tiwa, which is spoken (with some differences) at Picuris, Isleta, and Sandia Pueblos and remains unwritten.

The multistory pueblo complex is likely quite similar today to what Capitan Hernando Alvarado saw when he was sent to Taos as part of the expedition of Francisco Vasquez de Coronado on August 29, 1540 to look for the fabled Seven Cities of Cibola. In fact, custom prohibits modern conveniences like electricity or running water in the old pueblo. Consequently, only about 150 people (of 1900 tribal members) live there year-round and many still obtain their potable water directly from the creek.

By 1598, Don Juan de Oñate, the first Governor of the territory that is now New Mexico established Spanish colonies with Catholic missions near most of the pueblos in Northern New Mexico. The Mission de San Geronimo, the first church at Taos

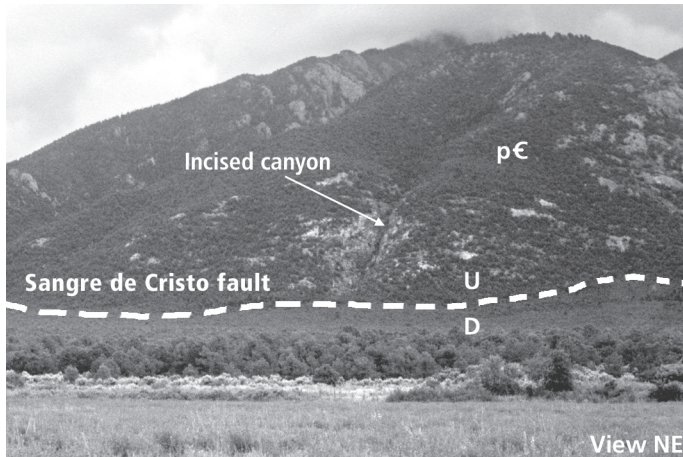


FIGURE 2.22. Photograph of the Sangre de Cristo range front northeast of Taos Pueblo, showing uplifted Proterozoic rocks, and faulted Pleistocene alluvial-fan deposits west of the fault. Note the dramatic incised bedrock canyon that has no corresponding arroyo in the hanging wall Quaternary alluvial fans.

Pueblo, was built sometime between 1610 and 1619. By 1615, settlers had moved to Ranchos de Taos (originally Las Trampas de Taos) to farm the floodplain of the Rio Grande del Rancho.

In 1680, growing conflicts between the pueblos and the Spaniards culminated with the Pueblo Revolt which was organized by Popé, a native of San Juan Pueblo who was in hiding at Taos Pueblo. The natives were unwilling to tolerate the subversion of their native religion and the *Encomienda* (a tribute payment to a Spanish landowner 'commended' with the spiritual and physical well-being of those in his charge but what essentially amounted to slavery). This was the most successful anti-colonial uprising in the history of the continent. After 13 years, Don Diego de Vargas re-conquered New Mexico. However Taos Pueblo resisted Spanish occupation of the valley until 1696.

Though long a destination of nomadic traders prior to colonization, a decree by the Spanish government in 1723 forbid trade with the French entirely and trade with the plains Indians only through Taos and Pecos. This led to the annual summer Taos trade fairs, which drew people, native and non-native alike, from half the continent. At their peak, the governor of the province would declare a *Pax de Dieu* or 'Peace of God', which suspended all warfare for the duration of the fair. French trappers and other mountain men were drawn to the fairs to trade for pelts and added excitement and color, especially after consuming 'Taos Lightning,' a whiskey produced at Simeon Turley's mill in Arroyo Hondo (see Day 1 log).

The Mexican-American War arrived in New Mexico in 1846 when General Stephen Kearny marched into Santa Fe with no opposition. However, insurgents in Taos opposed to American occupation killed the first Territorial Governor, Charles Bent (who's house is now a museum on Bent Street near the plaza) and others sympathetic to the Americans. The U.S. Army marched north from Santa Fe to the church at Taos Pueblo, where the insurgents were fortified, to put down the Taos Rebellion. The ensuing bombardment destroyed the original San

Geronimo mission and killed some 150 people. The church was rebuilt in 1850.

In 1848, the Treaty of Guadalupe Hidalgo was signed, ending the Mexican-American war with the United States in possession of what is now the Southwest. By treaty, the Spanish and Indian Land Grants were honored by the United States. However, significant conflict continues to this day regarding land grant issues, particularly with regard to common grant lands used communally for grazing and other forest resources that were lost to the U.S. Government. This happened in 1906 to Taos Pueblo when mountainous lands to the east became National forest. In 1970, President Nixon returned some 48,000 acres of this federal land considered sacred to Taos Pueblo, including Blue Lake, which is central to their traditional ceremonial rites. Ironically, being conquered by the Spanish afforded the pueblos more protection for land and culture than most other tribes outside New Mexico whose first European contact was with English or French colonists or their descendants. This protection has assured the pueblos a relatively peaceful coexistence with non-natives since 1848.

See the Taos Pueblo website: <<http://www.taospueblo.com>> for more information on history culture, festivals, and other events at Taos Pueblo.

See the Taos Historical Society website for more on the history of Taos: <<http://www.taos-history.org>>

Return to vehicles and retrace route back towards Taos.

- 14.4 Cerro Pedernal is visible at 1:30; Cerro Azul visible in middle distance in front of the Jemez Mountains. 0.5



FIGURE 2.23. Photograph of the north house of the ancient Pueblo of Taos. The two main adobe buildings, separated by the Rio Pueblo de Taos (aka Red Willow Creek), are called *Hlauuma* (north house) and *Hlaukwima* (south house). They are considered to be the oldest continuously inhabited communities in the country. Taos Pueblo is the only living Native American community designated both a World Heritage Site by UNESCO and a National Historic Landmark. The multi-storied adobe buildings have been continuously inhabited for over 1000 years.

15.9 The paved road on the left leads to the site of Optional Stop 4. ACCESS IS BY PERMISSION ONLY. Under no circumstances should anyone enter Tribal lands without permission from the Tribal government. **1.5**

OPTIONAL STOP 4. The old windmill site east of [33] the Indian Health Clinic.

(Mileages for stops on the Pueblo are not included in this log.)

At this stop we examine a Sangre de Cristo fault scarp, and view the site of a 2003 trench across the scarp.

Geologic mapping of faults and fault scarps:

Machette and Personius (1984) and Personius and Machette (1984), mapped the Quaternary traces of the southern Sangre de Cristo fault along the mountain front east of Taos. Menges (1988, 1990) refined this mapping and interpreted the presence of multiple rupture segments that coincide with a similar pattern of segmentation of the Sangre de Cristo Mountain range. These workers noted fault scarps as much as 18 m high, and interpreted the occurrence of multiple late Quaternary surface ruptures. Subsequent detailed field and air-photo mapping of fault strands (Fig. 2.24) and late Quaternary surficial deposits provide additional information on the pattern of faulting (Bauer and Kelson, 2001). For example, the moderately west-sloping piedmont along the Sangre de Cristo mountain front contains a coalescent alluvial-fan complex that consists primarily of coarse deposits derived from Pennsylvanian-age bedrock in the Sangre de Cristo Mountains (Bauer and Kelson, 2001). Along this piedmont, the western fault strand is associated with scarp heights that range from 3 ± 1 m to 9 ± 1 m on three separate alluvial-fan surfaces (Kelson et al., 2003). These data suggest the occurrence of multiple surface ruptures along this fault strand over the past several tens of thousands of years or more.

2003 fault trench:

The Taos Pueblo site (Fig. 2.25) was chosen for investigation because it has: (1) excellent geomorphic relations that constrain

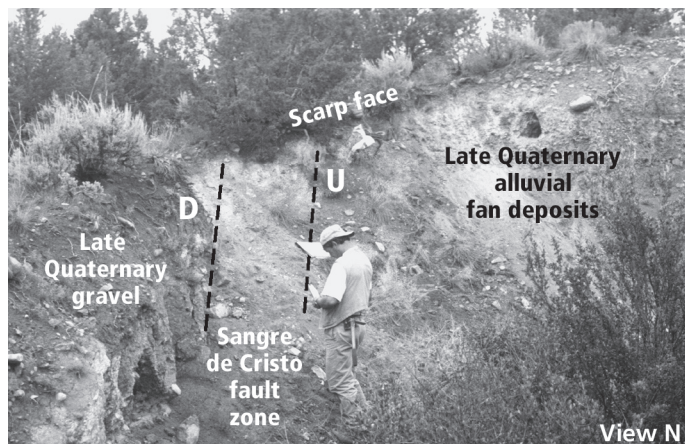


FIGURE 2.24. View north of an arroyo exposure of the Sangre de Cristo fault northeast of Taos. The scarp is interpreted as having been repeatedly active in late Quaternary time. The fault dips steeply west.

the location of the main strand of the fault; (2) has late Pleistocene alluvial-fan deposits on the mountain-front piedmont; and (3) there is minimal cultural disturbance (Plate 9; Kelson et al., 2003; Kelson et al. 2004b, this volume). The primary goals of the trench were to provide information on (1) large, geologically recent earthquakes along the southern Sangre de Cristo fault on Taos Pueblo lands, and (2) document fault characteristics in the shallow subsurface to help evaluate influences of the fault on vadose zone groundwater flow.

Detailed topographic surveying of the trench site shows that the primary fault scarp across the late Pleistocene alluvial fan exhibits about 3 m of net vertical tectonic displacement. Progressively greater amounts of displacement of older alluvial fan surfaces suggest that the fault has produced multiple surface ruptures within the past several tens of thousands of years or more. In addition, a distinct bevel in the scarp profile at the trench site suggests the occurrence of two surface ruptures since deposition of the alluvial fan, each with about 1.5 m of vertical displacement. These displacements are consistent with large earthquakes having magnitudes in the range of M6.5 to M7.5 (Kelson et al., 2003; Kelson et al. 2004b, this volume).

Stratigraphic relations exposed in the trench show the presence of middle to late(?) Pleistocene eolian and alluvial-fan deposits on the western, upthrown side of the fault, and probable late Pleistocene alluvial and colluvial deposits on the eastern, downthrown side of the fault. With the exception of the presently active colluvium, the deposits are not correlative across the fault. Stratigraphic evidence of surface-fault rupture is restricted to a package of scarp-derived colluvium on the downthrown side of the fault. This colluvial package includes fissure-fill and near-scarp deposits that probably were deposited immediately following the surface rupture. We interpret that the moderately developed soil formed on this colluvial package, including a soil Btk horizon and stage I calcium carbonate accumulation, is about 10,000 to 30,000 years old. Thus the trench exposure at the Taos Pueblo site suggests that the most-recent surface rupture along the southern Sangre de Cristo fault occurred about 10,000 to 30,000 years ago. Geologic evidence of previous faulting also exists in the form of well-developed fault gouge, more than 3 m of stratigraphic displacement, and fault-scarp morphology, but the timing of this deformation is unconstrained.

The main fault strand at the trench site is located near the base of the topographic scarp, and consists of a primary west-dipping fault plane and secondary faulting within a 6-m-wide zone on the hanging wall. The primary fault zone contains multiple anastomosing strands within the sheared alluvium, with strands commonly bordering lentic-shaped bodies of sediments. The pervasive shearing within the fault zone probably represents a zone of comparatively lower permeability, and the bulk permeability likely is anisotropic with greater permeability down the fault zone rather than across it. Several near-vertical fractures within the fault zone are associated with calcium carbonate accumulations, suggesting that downward percolation of meteoric water occurs preferentially along these fractures. The trench shows the presence of calcium carbonate cementa-

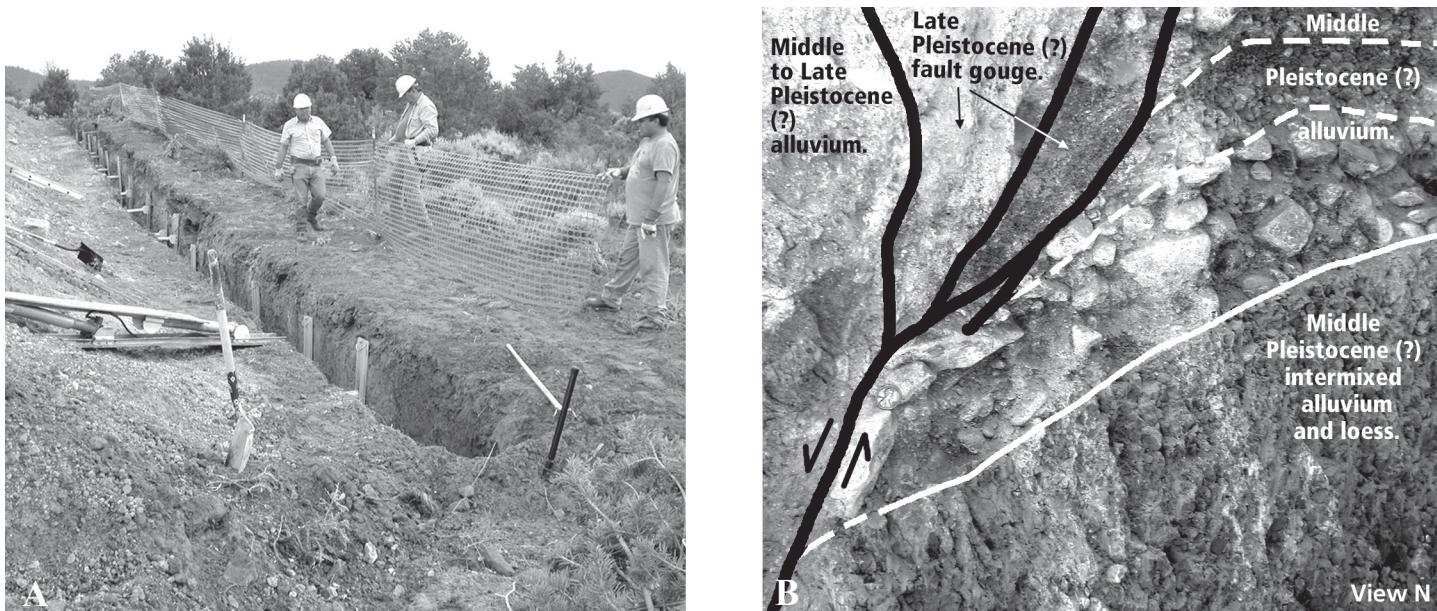


FIGURE 2.25. Photograph (A) of the 2003 Taos Pueblo fault trench on a segment of the Sangre de Cristo fault. See paper by Kelson et al. (2004b, this volume) and Plate 9 for a full description. A close-up (B) of the primary fault exposed in the north wall of the trench shows Middle to Late Pleistocene(?) gravel of the hanging wall against deflected and attenuated Middle Pleistocene (?) gravel beds of the foot wall, with a wedge of Late Pleistocene(?) fault gouge between.

tion commonly along fault planes in fine- and medium-grained deposits, as well as intersecting patterns of sub-horizontal and sub-vertical accumulations that likely are related to vadose-zone groundwater processes. The cementation locally observed along the fault exposed in the trench may be indicative of preferential groundwater flow down dip along the fault.

**Return to vehicles.
Backtrack to entrance to Taos Pueblo.**

- 16.0** Stop sign at gas station. Turn left on US-64 towards Taos Plaza. **0.1**
- 16.4** Kit Carson Park on left just before the stoplight for Civic Plaza (see *Minipaper by McLemore*). **0.4**
- 16.5** Historic Taos Inn on the left. Bent Street on right leads to several shops and former territorial Governor Charles Bent's house, now a museum, where he was murdered by those opposed to U.S. occupation of the territory. **0.1**
- 16.5** Continue straight through light. Taos plaza is a block to the right. The older parts of the Town of Taos, including the plaza, are on the middle Pleistocene Qt2 alluvial terrace formed at the confluence of the Rio Pueblo de Taos and the next drainage to the south, the Rio Fernando de Taos. This is the highest alluvial terrace remnant along either of these streams, and probably was attractive to early settlers because of the views and relatively dry high ground. This surface correlates with other remnants of the Qt2 terrace, which are inset into the highest aggradational surface on the Taos Plateau (the Qf1 fan surface, Bauer and Kelson, 2001). **0.0**

- 16.6** Descend from the Qt2 terrace onto a low, Holocene terrace flanking both sides of the west-flowing Rio Fernando de Taos. There are many springs and groundwater is shallow along the perennial Rio Fernando de Taos in this area. **0.1**
- 17.3** Ascend onto the Qfu fan surface, a coalescent alluvial-fan complex derived from drainages along the Sangre de Cristo Mountain front. This map unit includes middle to late Pleistocene fans that have well-developed soils with stage III to IV carbonate accumulation, and are graded to the Qt2 to Qt4 terraces along Rio Pueblo de Taos. Locally, younger alluvial fans (unit Qfy, Bauer and Kelson, 2001) are inset into the Qfu fans. The Qfy fans have moderately developed soils, including stage I to II carbonate accumulation, and are graded to the Qt6 and younger alluvial surfaces along Rio Pueblo de Taos. **0.7**
- 17.6** Stoplight at La Posta Rd. Over the next 2 miles or so, our route traverses the Qfu alluvial-fan complex, which has irregular topographic relief because of multiple fan lobes and incised arroyos. **0.3**
- 17.8** Stoplight at Cruz Alta Rd. **0.2**
- 18.0** Sun God Lodge on left was used in the 1988 Hollywood production *Twins*, starring Arnold Schwarzenegger and Danny DiVito. **0.2**
- 18.6** Stoplight at Paseo de Cañon. The sublime Picuris Mountains are on the skyline at 12:00. **0.6**
- 19.4** Sagebrush Inn is on the right. **0.8**

Kit Carson Memorial Park and Cemetery

Virginia T. McLemore,

New Mexico Bureau of Geology and Mineral Resources, New Mexico Tech, Socorro, NM 87801

Kit Carson Memorial Park and Cemetery, located in the center of Taos, is unlike most cemetery areas. It is not a somber place, but a vibrant tribute to the colorful life of frontiersman and scout Kit Carson. With picnic areas, playgrounds, a baseball field, basketball and tennis courts, bicycling/walking trails winding through a stand of cottonwoods, and even an ice-skating pond in winter it is an urban park filled with cheerful sounds. Markers identify various plants and explain local historical features of the park. Restrooms are available, but overnight camping is not allowed.

The park, which consists of only 19 acres, was established in 1949 on what was then the edge of town. The park was part of the New Mexico State Parks Division until 1992, when it was turned over to the city of Taos. It is a popular park with annual visitation totaling 150,000-260,000. Today the park lies north of the Taos Plaza, a cultural and tourist center with museums and historical monuments reflecting Indian, Spanish, and American cultures.

The park is the final resting place of Christopher “Kit” Carson and his family. His grave is marked with a *cerquita* (a spiked wrought-iron rectangular fence), traditionally used to outline and protect burial sites. Also interred here is Mabel Dodge Luhan, the pioneering patroness of the early Taos art scene.

Kit Carson was born in Madison County, Kentucky in December 24, 1809. When he was 17, he joined a wagon train headed for Santa Fe. As a young man, he became an accomplished hunter, trapper, guide, scout, soldier, Indian agent, and courier. He had a remarkable sense of direction and traveled across the continent several times prior to the arrival of stagecoaches, railroads, and most wagon trains. In 1842, 1843, and 1848, he scouted for Captain John C. Fremont. Kit Carson married a Taos girl, Maria Josefa Jaramillo, in early 1843, but family life was not enough to keep him from traveling. In 1846 he guided General Kearney’s army during the Mexican War. Afterwards, he settled on a farm at Rayado, south of Cimarron, near Lucien B. Maxwell’s home. Both homes are preserved by the Boy Scouts of America on the Philmont Ranch.

REFERENCES

- Estergreen, M. M., 1929, Kit Carson, a portrait of courage: University of Oklahoma Press, 3rd edition, 320 p.
 Utley, R. M., 1962, Fort Union National Monument: National Park Service, Historical Handbook 35, 68 p.
 Vestal, S., 1928, Kit Carson, the happy warrior of the Old West: Riverside Press, Cambridge, 297 p.
 Young, J. V., 1984, The state parks of New Mexico: University of New Mexico Press, Albuquerque, 160 p.

20.0 Continue past NM-518 on left. The highway descends from the Qfu fan complex into the Rio Grande del Rancho valley. **0.6**

20.4 San Francisco de Assisi Church on left. This church rests on a remnant of the late Pleistocene Qt4 terrace, formed by the Rio Grande del Rancho. (See Sidebar 2.1) **0.4**

Farming did not appeal to him and in 1854 he accepted an appointment as Indian Agent for the Ute, Apache, and Pueblo Indians, which he held until 1862. In 1862 he joined the Union army and helped organize the 1st New Mexican Volunteer Infantry of the Union Army. He fought Confederate forces at the Battle of Val Verde in central New Mexico and led several successful campaigns against hostile Indians. In 1863, he was ordered to relocate the Navajo and Mescalero Apache Indians to the Bosque Redondo Reservation at Fort Sumner. The project, designed to turn the Indians into farmers, failed. The tribes were returned to their original homes within a few years, but not before they had suffered starvation and many deaths. In 1865 Carson was given a commission as brigadier general and cited for gallantry and distinguished service. After the war Carson served as the commanding officer at Ft. Craig and Ft. Union, New Mexico, and Ft. Garland, Colorado. He was mustered out of the army on November 22, 1867 (Utley, 1962).

Throughout his travels and adventures, Kit Carson thought of Taos as his home and spent much of his time there. His Taos home, not far from the state park, is now a museum. On May 23, 1868, 59-year-old Kit Carson died of natural causes at Fort Lyon, Colorado, only months after his wife died during childbirth. Their bodies were moved to Taos and buried at the present site according to their prior request (Vestal, 1928; Estergreen, 1979; Young, 1984). Teodora Martinez Romero donated the land for the cemetery in 1847 for the burial of American soldiers and civilians killed during the Taos Indian Rebellion. Subsequently, several prominent citizens of Taos and local soldiers who served in the Mexican War, the Indian campaigns of the 1850’s, the Civil War, the Spanish American War, and World Wars I and II were buried at the cemetery.

Kit Carson Memorial State Park and Cemetery offers a refreshing contrast to the nearby tourist attractions around and near the Taos plaza. While resting in the midst of some of the most spectacular scenery and geology in northern New Mexico, the park visitor can relax, picnic, stroll through the park, and reflect upon the wild west days of Kit Carson.

20.5 Crossing the Rio Grande del Rancho. The headwaters of this stream are eroding Pennsylvanian sandstone and shale as well as subordinate amounts of volcanoclastic rocks from the Tertiary Picuris Formation. The present-day, shallow-gradient channel meanders across the broad, flat-floored valley, in contrast to the steep, straight channels typical of streams draining crystalline rocks north of Taos (i.e., Rio Hondo and



FIGURE 2.26. During the summer of 1999, 31 members of NASA's 1998 astronaut candidate class participated in geophysical training exercises in the Taos area. They collected detailed gravity data in the southern Taos valley in order to identify buried Sangre de Cristo faults for an ongoing hydrogeologic investigation. The gravity method was used on the Moon by Apollo 17 lunar explorers, and may be a useful technique for other planetary exploration—particularly of Mars, where windblown sand mantles a highly varied terrain. The discovery of magnetic stripes on Mars, perhaps analogous to those that record seafloor rifting on Earth, raises the possibility that gravity surveys might reveal significant buried martian structures. In this photograph, veteran Apollo 16 lunar explorer and space shuttle commander John Young (center) evaluates the training exercise while astronaut candidates Chris Ferguson and Barbara Morgan take gravity and GPS readings.

Rio Lucero). The present-day discharge is dominated by relatively low peak discharges, and the present-day bedload consists nearly completely of sandstone pebbles and cobbles. At the mouth of Rio Grande del Rancho canyon is the village of Talpa, where the west-down Sangre de Cristo fault on the north merges with the northwest-down, left-lateral Embudo fault zone. **12.1**

20.8 Turn left onto NM-382 into the community of Llano Quemado (“burnt plain”) that was first mentioned in church records in 1787 (Cash, 1993). Note Qt2 gravels in steep roadcut on right. We are driving along the Qt2 terrace of the Rio Grande del Rancho, which is associated with pebble and cobble gravel and a well-developed soil exhibiting stage III soil development. **0.3**

21.0 Road ascends onto the top of the broad, northwest-sloping Qt2 surface. **0.2**

21.1 Church on left is Nuestra Señora de Carmen, built in 1940. **0.1**

21.7 Stay right on gravel Miranda Canyon Road at fork. [35] We are ascending the Qf2 alluvial fan, which is graded to the Qt2 terrace near Llano Quemado. **0.6**

22.0 Just ahead, past the (defaced) Miranda Grant sign (Fig. 2.28), is a subtle slope break that represents a



FIGURE 2.27. The back of the San Francisco de Assisi church is reportedly one of the most photographed and painted churches in the country. Another photo of the church by Dana Ulmer-Scholle.

SIDEBAR 2.1 — San Francisco de Assisi Church:

Completed in 1810 (but perhaps as early as 1776 according to some historians; Cash, 1993), this massive adobe structure has walls that are ~13 feet thick at their base. It is considered to be one of the finest examples of Spanish mission architecture in the Southwest, and is perhaps the most photographed and painted church in the country (Fig. 2.27). This fortress-like architecture reflects Indian tribes' resistance to conversion to Christianity. Periodically, parishioners maintain the exterior by replastering with a mixture of adobe mud and chopped straw. Most old adobe buildings have been plastered over with concrete or synthetic stuccos. In fact, the church was hard-plastered in 1967 but this was removed in 1979 (Cash, 1993). The soft curves of the distinctive buttresses and mud plaster gives this church a very pleasing appearance, especially at sunset. **-12.0**



FIGURE 2.28. This curiously incomplete sign, which surely precipitated the deposition of the old couch, sits on a degraded mid-Pleistocene Embudo fault scarp at Mile 22.

degraded mid-Pleistocene fault scarp (Bauer et al., 1999b). This is the northern-most scarp within the 2-km-wide Embudo fault zone near Talpa, and probably is part of the structural transition from the left-lateral Embudo fault zone on the southwest to the west-down Sangre de Cristo fault on the north. A small quarry to the left displays soil developed on the Qfz (Fig. 2.29). **0.3**

22.2 At 9:30, behind the ridge, at the base of the mountain, is the location of Ponce de Leon hot spring (93°F), named for the Spanish explorer and soldier who sought the fountain of youth in Florida in the early 1500s. The spring was once developed with multiple large pools as part of a resort that fell into disrepair. The Taos Land Trust now controls the spring and surrounding area, but it is currently closed to the public. The spring is located in Proterozoic granitic rock, and appears to discharge at a zone of intersection between a thick pegmatite and a Laramide(?) brittle fault (Bauer et al., 1999b). **0.2**

22.5 The round hill that sits in the middle of the valley ahead is an erosionally resistant outcrop of Llano Quemado rhyolite breccia of the Picuris Formation. It is flanked on the east and west by north-striking, high-angle faults that have Laramide characteristics, but cut rocks that are as young as Miocene. We will visit that hill at Stop 5b. **0.3**

22.7 STOP 5. La Serna Land Grant

[36] Turn right before Serna Grant fence line and park.

This federal land is part of what is claimed as the La Serna Land Grant, however, recent court rulings have rejected that claim. In the recent past, access was only allowed with permission from La Serna Grant Board (since dissolved). However, this issue may resurface, so be sure to check on current access constraints. At this stop we will walk to a well-exposed segment of the Embudo fault zone, outcrops of the Picuris Formation including the Llano Quemado breccia, and Laramide-style strike-slip faults of the Miranda graben that cut Oligocene strata. **0.2**

STOP 5a—Embudo fault exposure.

[37] Walk west into the arroyo.

Proceed along the arroyo that parallels the dirt road and then southeast up the first tributary drainage on the left to a rare exposure of a strand of the Embudo fault.

A fault triple-point at Talpa:

Three major fault systems intersect (Fig 2.30) in the southeastern corner of the Taos Plateau: 1) the Picuris-Pecos fault system—see below; 2) the Embudo accommodation zone fault zone; and 3) the rift-bounding Sangre de Cristo fault zone. Additionally, a 7-km-wide zone of west-down faults, originally mapped by Lambert (1966) and termed Los Cordovas faults by Machette and Personius (1984), exist on the plateau along the northern projection of the Picuris-Pecos fault (see Day 1, Stop 1). The



FIGURE 2.29. This soil is well exposed in a small quarry just east of the road at mile 22. The photo shows the upper 40 cm of an alluvial fan deposit with an eolian component and a weakly developed A horizon, which overlies a buried fine-grained alluvial fan deposit. The lower fan deposit contains a moderately developed Btk soil horizon and a well-developed Bk (Stage III) calcic horizon. These soil characteristics, and inset relations with other deposits in the area, suggest a mid-Pleistocene age for the Qf2 map unit. Dirt geologists “hammer” for scale.

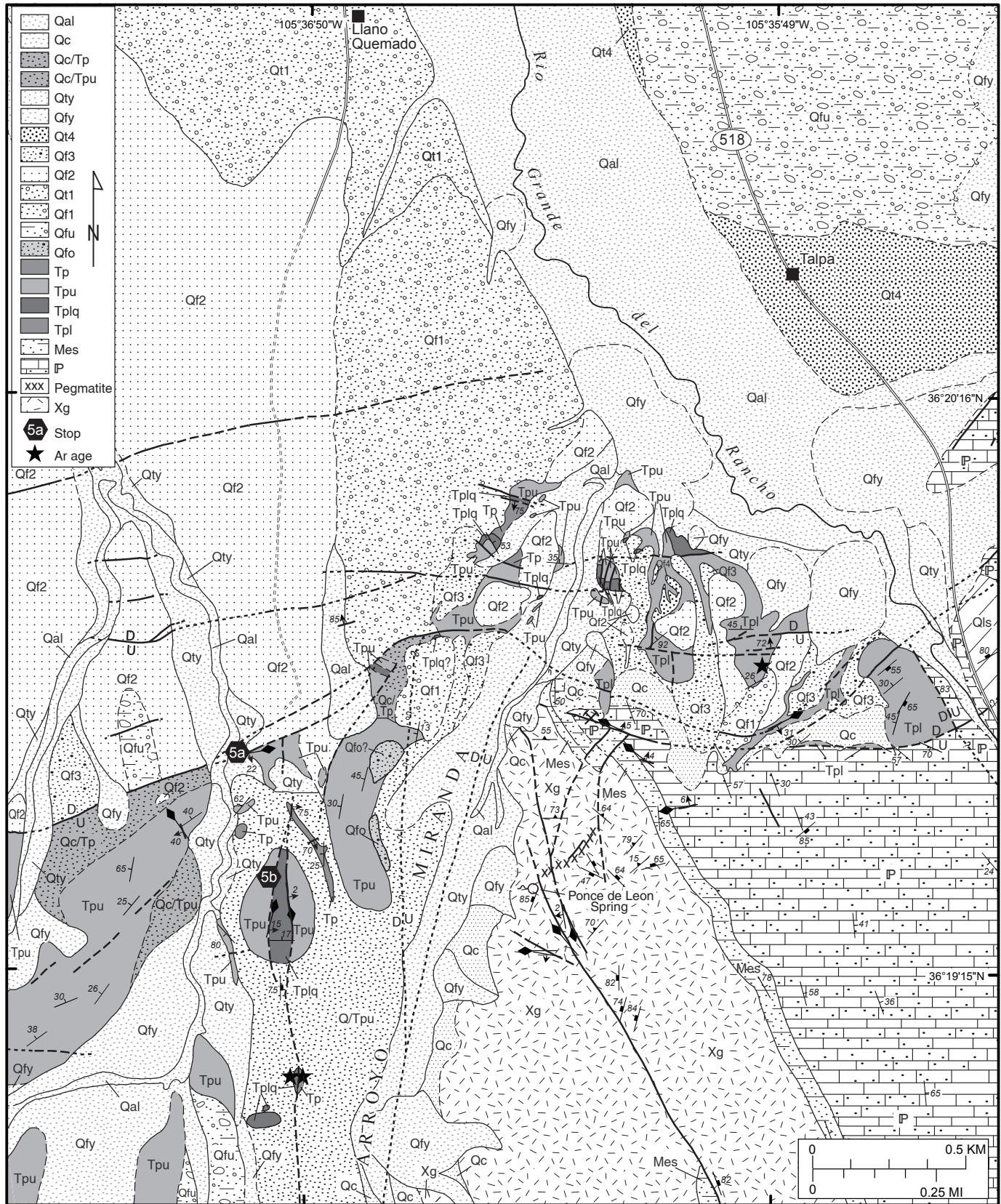


FIGURE 2.30. Geologic map of the Miranda graben area, modified from Bauer et al. (1999b) and Bauer and Kelson (1997). The Picuris-Pecos fault system consists of a number of large-displacement, north-striking, high-angle faults that juxtapose Proterozoic, Paleozoic, and Tertiary rocks in a series of horsts and grabens. The Miranda graben is the westernmost Tertiary-filled graben in the geologically complex zone between the Picuris and Sangre de Cristo Mountains.

geometries and kinematics of all four of these fault zones provide insight into the geometry and history of the southeastern San Luis Basin (Bauer and Kelson 2004a, this volume).

The corner of a rift basin—the intersection of the southern Sangre de Cristo fault and the northern Embudo fault:

The Sangre de Cristo and Embudo fault systems form the eastern and southern boundaries of the San Luis Basin, respectively, and intersect in a manner characteristic of continental rift systems (Rosendahl, 1987; Morley et al., 1990). The Sangre de Cristo fault is a north-striking, west-dipping normal fault that accommodates asymmetric subsidence of the late Cenozoic San Luis Basin (Fig 2.31). The Sangre de Cristo fault exhibits geomorphic evidence for multiple surface-rupturing events in the late Quaternary (Machette and Personius, 1984; Menges, 1990).

The 64-km-long Embudo fault strikes northeast, and can be interpreted as a transfer fault or accommodation zone (Rosendahl, 1987; Morley et al., 1990; Faulds and Varga, 1998) that allows differential subsidence between the San Luis Basin to the northeast and the Española Basin to the southwest. Detailed field mapping and geomorphic investigations document late Quaternary and possibly Holocene surface rupture along the northeastern Embudo fault (Kelson et al., 1997, Kelson et al., 2004a, this volume). The Embudo fault is an excellent example of an active accommodation zone in the northern Rio Grande rift.

Description of the Embudo fault system transfer zone:

The Embudo fault zone is a sinistral accommodation zone that forms the border between the west-tilted Española Basin and the east-tilted San Luis Basin of the Rio Grande rift. The 64-km-long fault links the west-down southern Sangre de Cristo fault with the east-down Pajarito fault, and appears to be a high-angle fault with different senses of vertical separation along strike (Kelley, 1978; Muehlberger, 1979; Leininger, 1982; Machette and Personius, 1984; Kelson et al., 1997, Kelson et al., 2004a, this volume; Koning et al., 2004b, this volume). The fault is thought to be part of the Jemez lineament, a regional structural/volcanic trend that may have been a zone of crustal weakness since late Precambrian time (Muehlberger, 1979).

Seismic potential of the Embudo fault:

The seismic potential of transfer zones in active rifts is poorly understood, with no known historical examples of surface-rupturing earthquakes along structures that trend obliquely across rifts. Detailed geologic mapping along the 35-km-long northeastern section of the Embudo fault shows evidence of late Pleistocene and possibly Holocene displacement along many discontinuous fault strands that are distributed over a width of several kilometers (Kelson et al., 1997; Bauer and Kelson, 1997). There are substantial variations in the heights of fault scarps along strike, that, in conjunction with subhorizontal slickensides on fault planes and reverse faulting within a right stepover, suggest that the northeastern section of the Embudo fault has had left-oblique slip during the Quaternary.

Where scarps are present along the northeastern section of the fault, scarp heights appear to correlate with local strikes

of fault strands, with more northerly strands exhibiting prominent scarps and more westerly strands having low scarps and discontinuous expression. These relations are consistent with roughly east-west extension across the rift, and left-lateral slip on the northeastern Embudo fault, rather than reverse slip as previously postulated. Because of considerable structural complexities along the fault and the reversal in the sense of vertical separation near the town of Embudo, it is unlikely that the entire 64-km-long Embudo fault would rupture during a single, large-magnitude 6 earthquake. The most realistic rupture scenarios are individual ruptures on either the 35-km-long northeastern fault section or the 30-km-long southwestern fault section. The maximum magnitude earthquakes for these scenarios are estimated to be M 6.8.

Age and origin of the Embudo fault system:

Previous workers have suggested that the Embudo fault zone is a relatively young rift feature that corresponds with the initial uplift of the Picuris Mountains in the late Miocene (Manley, 1978; Ingersoll et al., 1990). Our recent mapping shows that there is no distinct boundary between the Embudo fault zone and the Cañon section of the Sangre de Cristo fault zone (Bauer et al., 1999; Bauer and Kelson, 2004a, this volume). The Embudo zone (Fig. 2.32) swings smoothly northward in the Talpa area to merge with the Cañon section of the Sangre de Cristo fault. The most reasonable explanation is that the Embudo and the Cañon section faults are the same age. Kelson et al. (1997) suggested that the Embudo and Sangre de Cristo faults both exhibit evidence of possible Holocene activity. Thus, there are three ways to view the kinematic history: 1) the Embudo fault (and therefore the uplift of the Picuris Mountains) is older than late Miocene; 2) at least parts of the Sangre de Cristo fault zone are also young; or 3) some combination of both.

Our current working hypothesis is that the crescent-shaped Taos valley embayment, defined by the Hondo and Cañon sections of the Sangre de Cristo fault on the east and the eastern

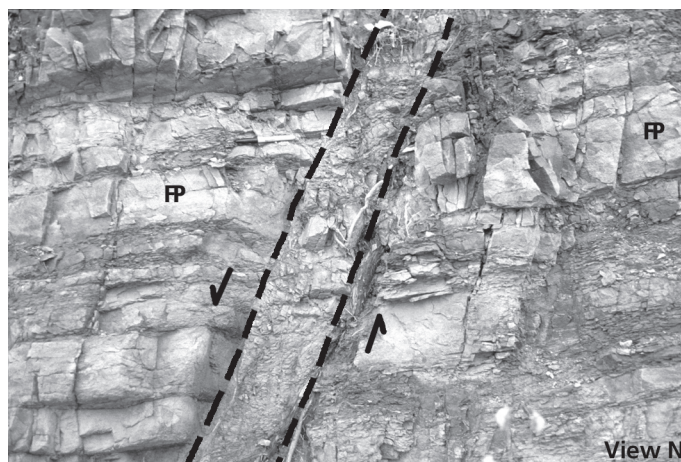


FIGURE 2.31. The Sangre de Cristo fault has pervasively fractured and faulted the Pennsylvanian bedrock around the southeastern and eastern edge of the San Luis Basin. This view north near Cañon shows a 20-cm-wide, west-dipping fault zone in Pennsylvanian sandstone.

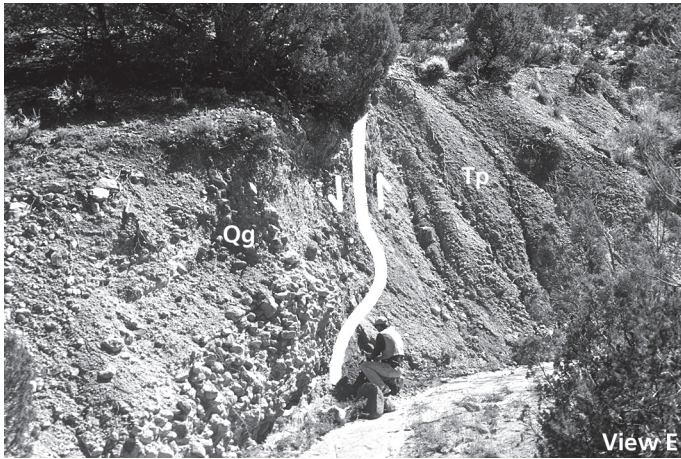


FIGURE 2.32. View east, along strike, of a major strand of the Embudo fault zone. In this unnamed arroyo, the site of Stop 5a, Quaternary gravel (Qg) is juxtaposed against Upper Picuris Formation pebbly sandstone (Tp) along a steeply north-dipping, left-lateral, north-down fault plane.

edge of the Taos graben on the west, formed contemporaneously with the Embudo transfer zone, in early Miocene time. If so, the pre-early Miocene eastern edge of the rift was defined, from north to south, by the Sangre de Cristo fault zone north of the Rio Hondo, the buried eastern edge of the Taos graben (i.e., Town Yard fault), and the Picuris-Pecos fault system of the Miranda graben.

STOP 5b—Picuris Formation.

[38] Walk upstream past the Embudo fault exposure. Take the first drainage on the left to get out of the arroyo. Head south and climb the small hill to view excellent outcrops of the Llano Quemado member of the Picuris Formation.

Picuris Formation:

The oldest Cenozoic unit in the area is the Picuris Formation; a local package of mostly volcanoclastic sedimentary rocks that represents pre-rift and early-rift activity (Fig 2.33; Table 2.1). It is thought that the early shallow rift basins of northern New Mexico were initially infilled by a combination of volcanic eruptions and volcanoclastic alluvial fans with sources in the San Juan volcanic field to the north (Baltz, 1978). The Picuris Formation probably represents such a deposit.

The only previous study of the Picuris Formation divided it into three members; the lower member, the Llano Quemado breccia member, and the upper member (Rehder, 1986). These subdivisions were made by examining and then correlating 11 scattered exposures. This work was a major contribution to understanding this important unit, but some interpretations are questionable due mainly to new isotopic ages and the remarkably extensive faulting present in the area. Although the Llano Quemado breccia is an excellent marker bed, in the Talpa area it crops out as a scattering of fault-bounded exposures that complicate straightforward stratigraphic reconstructions. A recent study by Aby et al. 2004 (this volume) compares and contrasts the Picuris Formation rocks exposed on the north and south flanks of the Picuris Mountains, and defines three regional members.

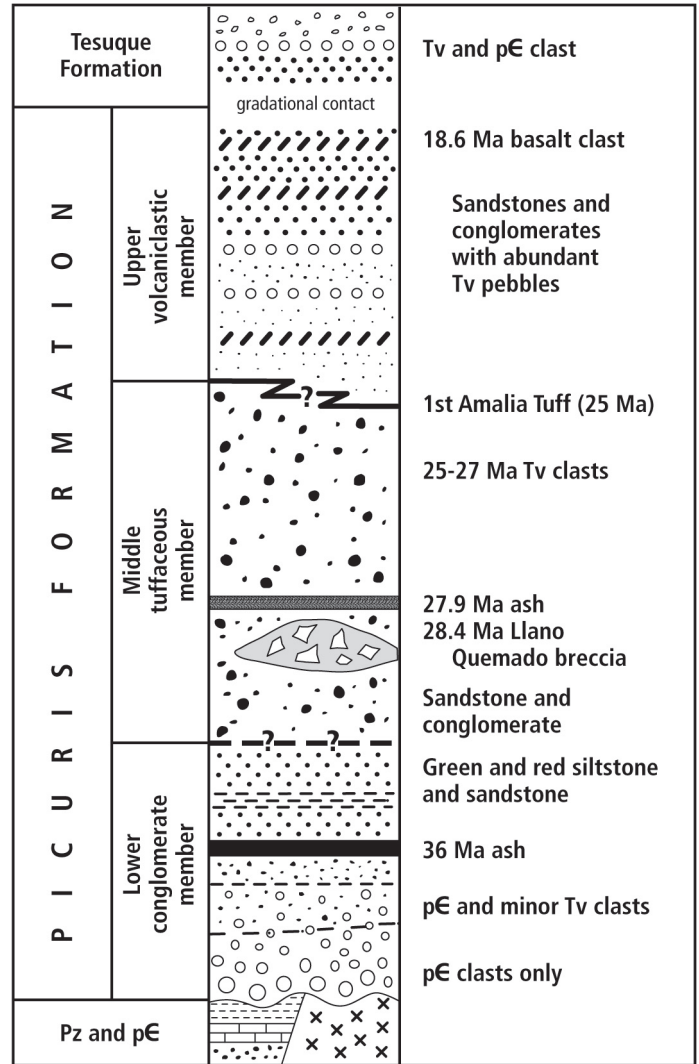


FIGURE 2.33. Generalized stratigraphic column for the Picuris Formation along the northern flank of the Picuris Mountains. Modified from Rehder (1986), Bauer et al. (1999b), Bauer and Kelson (1997), and Kelson and Bauer (1998).

Lower conglomerate member. The lower member of the Picuris Formation consists of a basal boulder and cobble conglomerate and conglomeratic sandstone interbedded with thinly bedded sandstones. The boulder unit is distinctive, composed of well rounded, poorly sorted, mostly clast supported, Proterozoic quartzite clasts, with minor altered clasts of intermediate Tertiary volcanic rocks and Paleozoic sedimentary rocks. The boulder unit grades (fines) upward to less indurated pebble conglomerate and conglomeratic sandstone, and variegated green, red, and white siltstone and mudrock. Local layers of primary(?) air-fall ash are well sorted and contain sanidine and biotite crystals.

This member was interpreted as a sequence of debris flow and alluvial fan deposits derived from the Sangre de Cristo Mountains and Latir volcanic field to the north and northeast (Rehder, 1986). However, the deposit (34 to 27 Ma) cannot be older than the Latir source (26 Ma), and therefore, the volcanic

Table 2.1. Results of recent ⁴⁰Ar/³⁹Ar geochronology of samples collected by P. Bauer and K. Kelson from the Taos Plateau and Penasco embayment. Analytical data from the New Mexico Geochronological Research Laboratory (McIntosh et al., 2004).

Ar/Ar Age (Ma)	Uncertainty (+/- Ma)	Unit Name	Rock Type Sampled	Description of Sample	Material Analyzed	7.5-min. Quad	UTM N (1927 NAD)	UTM E (1927 NAD)	Sample #	Comments
1.27	0.02	Qf1	ash	White ash, crossbedded, coarse & fine layers. Roadcut on NM-68.	15 sanidine crystals	Taos SW	4021630	438400	TaosSW-1	Reworked Plinian deposit from Jemez Mtns.
2.7	0.79	Servilleta Basalt	vesicular basalt	Basalt float from just S of airport. Local eruptive center?	groundmass concentrate	Los Cordovas	4033120	438608	LC-4.20.02-1	Float sample taken from surface. Ar loss. Altered.
3.06	0.33	Servilleta Basalt	massive basalt	Flow S of Rio Grande on Pilar cliffs. From top of flow.	groundmass concentrate	Trampas	4009683	424730	T-7.31.02-2	Fairly well-behaved spectra.
3.41	0.5	Servilleta Basalt	massive basalt	Flow S of Rio Grande on Pilar cliffs. From base of flow.	groundmass concentrate	Trampas	4009683	424730	T-7.31.02-3	Fairly well-behaved spectra.
5.44	0.2	Ocate Basalt	basalt	Mildly vesicular basalt outcrop from S of US Hill.	groundmass	Tres Ritos	4004600	444300	TresRitos-1c	Some alteration?
5.67	0.12	Ocate Basalt	basalt	Scattered basalt outcrops near Vadito.	whole rock	Penasco	4006190	437825	Pen-7.29.01-1	Minimum age.
18.59	0.7	Picuris Fm	basalt clast	D. McDonald basalt clast, upper mbr Picuris Fm., Miranda graben.	groundmass	Taos SW	4016380	443800	RdT-13	Disturbed spectrum, so minimum date.
20	?	Picuris Fm	basalt	Vesicular basalt clast, upper mbr Picuris Fm near top of hill 7551.	groundmass concentrate	Penasco	4007375	434565	Pen-2.18.03-1	Approximate age.
23.01	0.09	Picuris Fm	conglomerate	Pumice conglomerate, middle mbr Picuris Fm, top of Cerro Blanco.	8 sanidine	Penasco	4005963	439400	Pen-7.29.01-2	Mixed population. Maximum age.
23.707	0.042	Picuris Fm	pumice clasts	Pumice clasts in conglomerate, middle mbr, Picuris Fm.	8 sanidine	Penasco	4006609	437536	Pen-7.28.01-2	Good data. Single population. Maximum age.
25.16	0.1	Picuris Fm	volcanic cobble	Tv cobble in float in Picuris Fm, northern Picuris Mtns piedmont.	15 sanidine crystals	Taos SW	4018000	436250	PB-2	Probably San Juan volcanics
25.5	?	Picuris Fm	ignimbrite	Purple ignimbrite clast from middle mbr Picuris Fm, top of hill 7551.	28 small sanidine	Penasco	4007375	434565	Pen-2.18.03-2	Approximate age.
27.29	0.15	Picuris Fm	volcanic cobble	Tv cobble in float in Picuris Fm, northern Picuris Mtns piedmont.	single flake biotite	Taos SW	4018000	436250	PB-5	Probably San Juan volcanics
27.5	2	Picuris Fm	volcanic cobble	Tv cobble in float in Picuris Fm, northern Picuris Mtns piedmont.	single flake biotite	Taos SW	4018000	436250	PB-3	Poorly constrained age.
27.721	0.046	Picuris Fm	pumice clasts	Pumice-rich conglomerate, middle mbr, from S of Vadito Hill.	13 sanidine	Penasco	4005644	439738	Pen-7.29.01-5	Good data. Single population. Highly accurate eruptive age.
27.93	0.08	Picuris Fm	ash	White ash, poorly indurated, just below RdT-4 in Miranda graben.	15 sanidine crystals	Ranchos de Taos	4019200	444900	RdT-5	Good eruptive age.
28.03	0.08	Ancestral RG gravels	Tv clasts	Gravels from ancestral Rio Grande, west rim, S of Gorge bridge.	13 sanidines	Los Cordovas	4031000	435300	LC-4.19.02-1b	San Juan volcanic clast.
28.35	0.11	Breccia in Picuris Fm	rhyolite clast	White rhyolite clast. Llano Quemado breccia, Miranda graben.	15 sanidine crystals	Ranchos de Taos	4019200	444900	RdT-4	Good eruptive age.
34.5	1.2	Picuris Fm, lower mbr	ash	White ash near Pilar, lower mbr Picuris Fm, near Bradley conglom.	17 sanidine crystals	Carson	4013600	431070	Car-7	Confidence uncertain. Fine-grained. Sanidines altered.
34.64	0.16	Picuris Fm lower mbr	ash	10-cm white ash between lower red & greenish-gray claystones.	15 sanidine crystals	Ranchos de Taos	4020550	446350	RdT-8	Good eruptive age. Coarse-grained, so near source.
not datable		Picuris Fm	white ash	1-m-thick white ash from Hill 7551'.	no datable material	Penasco	4007320	434600	Pen-7.28.01-1	These two samples have similar chemistries, but are from different eruptions.
not datable		Picuris Fm	white ash	1.5-m-thick white ash from Cerro Blanco.	glass	Penasco	4005882	439270	Pen-7.29.01-3	
not datable		Picuris Fm	white ash	White ash, well indurated. Rehder's measured section B ash.	20 k-feldspar	Ranchos de Taos	4012450	448000	RdT-7	Xenocrystic, plutonic k-spar.
in progress		Servilleta Basalt	basalt	Very fine cuttings from West Deep well, Taos Pueblo.		Taos	4036110	447330	BOR-5. West Deep 1810-1830'	Based on microprobe geochemistry of phenocrysts (N. Dunbar, personal commun. 2003), these samples of borehole basalts are indistinguishable from the Servilleta Basalt.
in progress		Servilleta Basalt	basalt	Cuttings from BOR-6 well at 1050-1080 ft.		Taos	4035870	444960	BOR-6 1050-1080'	
in progress		Servilleta Basalt	basalt	Cuttings from BOR-6 well at 940-960 ft.		Taos	4035870	444960	BOR-6 940-960'	
in progress		Servilleta Basalt	basalt	Chips of Tertiary igneous rock, BIA Tract B (Tip) well, 660 ft.		Taos	4035793?	444827?	Tract B 660' Tip Well	
in progress		Servilleta Basalt	basalt	Chips of Tertiary igneous rock, BIA Tract B (Tip) well, 840 ft.		Taos	4035793?	444827?	Tract B 840' Tip Well	

component of the unit was probably derived from the older San Juan volcanic field to the north and northwest. Alternatively, the source could be a buried or eroded, unrecognized, older volcanic unit from the Latir field to the north.

Llano Quemado breccia. Llano Quemado breccia (Fig 2.34) is a light gray to red, monolithologic volcanic breccia of distinctive extremely angular, poorly sorted, light-gray, recrystallized rhyolite clasts in a generally reddish matrix. Rhyolite clasts contain phenocrysts of biotite, sanidine, and quartz. The rock is highly indurated and crops out as a ridge-former. The breccia was interpreted as a series of flows from a now buried, nearby rhyolite vent (Rehder, 1986). However, excellent exposures in Arroyo Miranda display layering and sedimentary structures such as crossbedding that indicate that at least parts of the unit are reworked volcanoclastic sediments, perhaps near-source primary surge deposits.

Upper volcanoclastic member. The upper member of the Picuris Formation is a gray to pinkish gray, immature, pumice-rich, ashy, polyolithologic, conglomeratic sandstone. It consists mainly of sandstones with gravel-sized clasts of pumice and silicic volcanic rocks (mostly 25.1 Ma Amalia Tuff), and minor Precambrian quartzite and intermediate composition volcanic rocks (including the 26.0 Ma Latir Peak quartz latite). Most of the gravel-sized fraction is pumice, with some clasts up to 25 cm in diameter. Most clasts are rounded to well rounded. Some cobble-rich conglomerates are interlayered with easily eroded, weakly cemented pebble conglomerates. Paleoflow measurements indicate a source to the north, and Rehder (1986) interpreted the unit as an alluvial fan deposit derived from the Latir volcanic field at about 26 Ma (Rehder, 1986). We agree, and would add that a new basalt clast date of 18.59 ± 0.70 Ma from the upper member (collected by D. McDonald) indicates that at least part of the section accumulated much later. Based on our



FIGURE 2.34. Typical Llano Quemado breccia member of the Picuris Formation at STOP 5b showing angular white rhyolite clasts in a reddish matrix. In this area, the breccia is found in a number of small, fault-bounded blocks that are strung out along Picuris-Pecos faults.

mapping along the northern Picuris Mountains piedmont, where the tilted, pedimented Tertiary rocks are locally exposed beneath Quaternary fans, we prefer to interpret a continuous section of Picuris Formation to Tesuque Formation, perhaps punctuated locally by unconformities.

Distribution of the Picuris Formation. Surface exposures of the Picuris Formation exist only west of the Rio Grande del Rancho. It is not known whether the Picuris Formation exists in the subsurface of the basin east of the Rio Grande del Rancho, but water well records do not support its presence there. Understanding the distribution of the Picuris Formation in the subsurface is important for hydrogeologic study because the Picuris Formation and the Santa Fe Group have dissimilar hydraulic properties. Whereas the basal conglomeratic and volcanic breccia units have the potential to store and transmit ample amounts of ground water, the overlying siltstone, mudstone, and immature middle ashy sandstone are expected to exhibit low to very low hydraulic conductivities (Bauer et al., 1999).

Picuris-Pecos fault system:

Montgomery (1953) recognized the Picuris-Pecos fault (originally named the Alamo Canyon tear fault) in the Picuris Mountains. The fault has been traced for more than 60 km, from the northern Picuris Mountains south of Taos, to near the village of Cañoncito, east of Santa Fe. From Cañoncito, it can be traced southward into the Estancia Basin for an additional 24 km, yielding a documented trace of 84 km.

Near its northern end, south of Taos, the Picuris-Pecos fault system consists of five, parallel, north-striking fault zones (Fig. 2.35). From west to east, they are: Picuris-Pecos, La Serna, Miranda, McGaffey, and Rio Grande del Rancho fault zones. Herein, these fault zones are collectively referred to as the Picuris-Pecos fault system. Each fault zone consists of high-angle, anastomosing zones of distributed brittle shear. The major faults form in valleys due to pervasive brittle deformational structures (fractures, fault gouge, fault breccia) that are relatively easily weathered and eroded. We suspect that all of the fault zones share similar kinematic histories of multiple reactivations, as described by Bauer and Ralser (1995).

The Picuris-Pecos fault is a major crustal boundary that has experienced enough slip to juxtapose very different Proterozoic rock packages. West of the fault is the Hondo Group, a thick metasedimentary section of quartzite and schist. East of the fault is a distinctive medium-grained, orange-colored granite (Miranda granite) that is similar in appearance to the granite exposed at Ponce de Leon spring. To the south, Paleozoic strata have been offset, indicating that the Picuris-Pecos fault has a Phanerozoic east-down separation. Slickenlines are typically strike-slip or shallow oblique-slip on steep fault planes.

Approximately 1.3 km east of the Picuris-Pecos fault is the east-down La Serna fault, which has placed the Miranda granite on the west against the Picuris Formation on the east. The Picuris Formation occupies a graben between La Serna fault and the west-down Miranda fault, located about 1.4 km to the east (see Minipaper by Kelly and McDonald and Nielsen, 2004, this volume). The main strand of the Miranda fault is inferred

LARAMIDE TO POST-LARAMIDE COOLING HISTORY OF THE MIRANDA GRABEN

Shari A. Kelley

Department of Earth and Environmental Science, New Mexico Institute of Mining and Technology, Socorro, NM 87801

The Picuris-Pecos fault system in the Sangre de Cristo and Picuris Mountains of New Mexico has been active in Proterozoic, Paleozoic, and middle Cenozoic time (Miller et al., 1963; Bauer and Ralsler, 1995; Kelley, 1995; McDonald and Nielsen, 2004, this volume; Bauer and Kelson, 2004a, this volume). The nature of possible late Mesozoic to early Cenozoic Laramide deformation along the fault zone has been more difficult to document due to a lack of preservation of synorogenic sedimentary rocks. In this reconnaissance study, apatite fission-track (AFT) thermochronology, which constrains the 60 to 110°C cooling history of rocks, is used to determine whether significant differential vertical motion and related exhumation occurred during early Laramide deformation across the 8-km-wide Picuris-Pecos fault system in the Miranda graben near the village of Talpa, New Mexico. This area was chosen because (1) the geologic structures are well mapped (Bauer and Kelson, 1997; Bauer et al., 1999b), and (2) the presence of the Picuris and Tesuque formations in the graben can be used to constrain the ~18 to 35 Ma history of the area (Bauer and Kelson, 2004a, this volume).

A total of ten samples were collected across the Picuris-Pecos fault system at the latitude of the Miranda graben; seven of these

samples yielded sufficient apatite for dating (Figure 2.35). Three samples were collected along a short traverse in the Proterozoic Miranda granite west of the La Serna fault, which juxtaposes the granite against the latest Eocene to Miocene Picuris Formation. Another traverse ran across Cuchillo del Ojo, an east-tilted fault block of granite east of the Miranda fault overlain by Mississippian and Pennsylvanian rocks. Two samples were also obtained from the Pennsylvanian sandstones on the east side of the Rio Grande del Rancho fault zone. In addition, two samples were collected on either side of the Picuris-Pecos fault in Telephone Canyon on the west side of the system just north of the Peñasco embayment (Figure 2.35).

The AFT data from the two higher elevation samples of Miranda granite west of the La Serna fault are similar, with ages of 52 to 54 Ma and relatively short mean lengths of 12.6 to 12.7 μm (Figure 2.35, Table 2.2). In contrast, the lowest elevation sample, which was collected about 50 m west of the fault breccia zone along the La Serna fault, is younger (43 ± 5 Ma) and has longer mean track lengths (13.6 ± 0.8 μm). These data suggest that differential vertical offset across the La Serna fault began in late Eocene time. A Miranda granite sample from the western

55th NMGS FFC 2004
Second-day Road Log

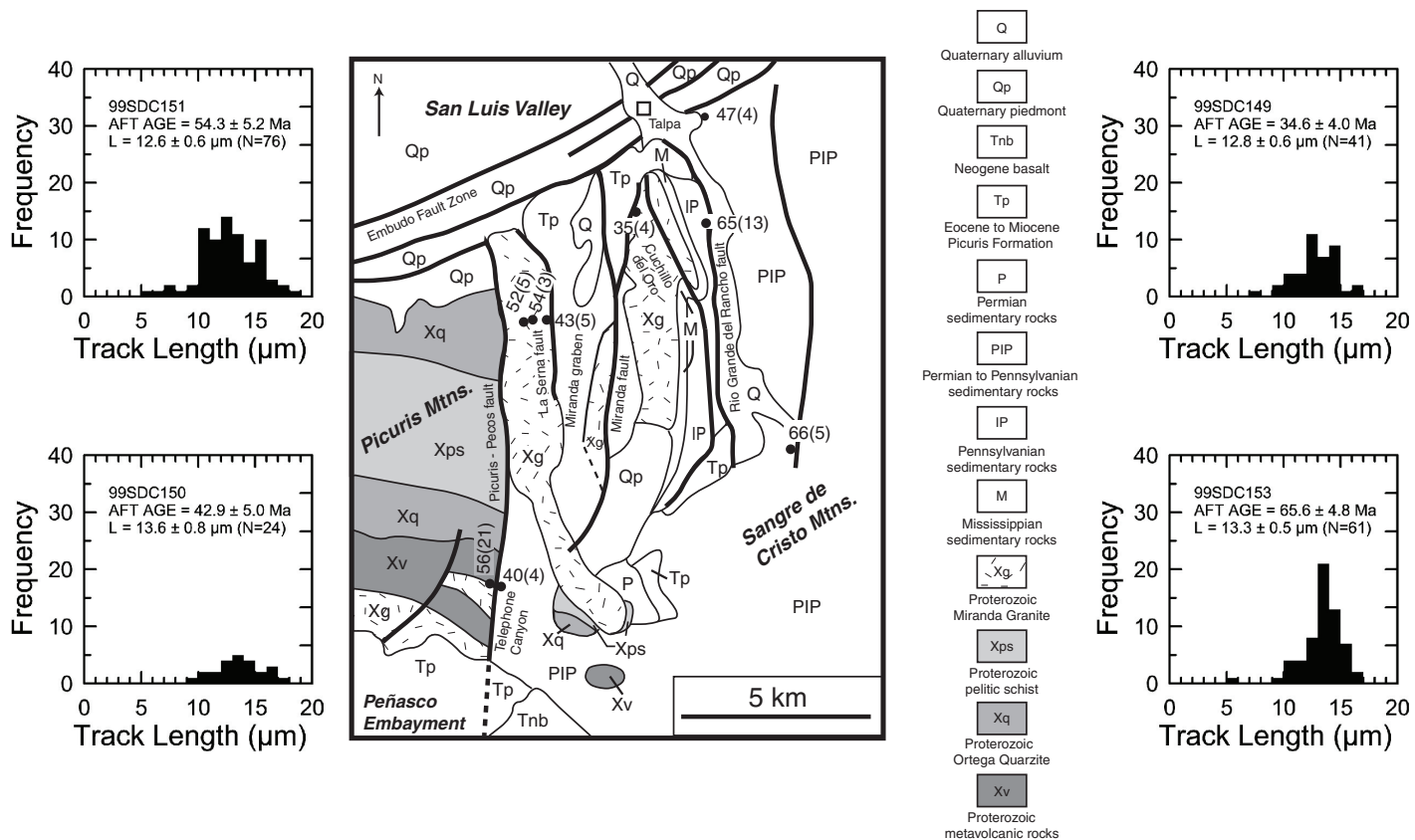


FIGURE 2.35. Simplified geologic map of the Miranda Graben modified from New Mexico Bureau of Geology and Mineral Resources Geologic Map of New Mexico (2003) and Bauer and Kelson 2004a (this volume). Faults illustrated as heavy black lines. Apatite fission-track sample localities represented by solid circles. AFT ages and standard error in the age is shown (in parentheses).

side of the Cuchillo del Ojo yielded a ~35 Ma AFT age. Short mean lengths of $12.8 \pm 0.6 \mu\text{m}$ imply a complex thermal history that possibly was influenced by the nearby Ponce de Leon hot spring. A sample of Pennsylvanian sandstone from the east side of the Cuchillo del Ojo has an AFT age of ~65 Ma. The small amount of apatite in this sample precludes track length analysis. The observed age trend across Cuchillo del Oro, with a younger age to the west, is consistent with the eastward tilt of the block. The Pennsylvanian sandstones to the east of the Rio Grande del Rancho fault system yield Laramide cooling ages. Age and track length data from sample SDC153 indicates that cooling in the Pennsylvanian section was in progress by ~66 Ma at a rate of ~2°C/m.y. The onset of cooling in the Pennsylvanian section to the north is slightly later (Fig. 2.35).

No statistically significant difference in AFT age is observed across the Picuris-Pecos fault in Telephone Canyon. These results are consistent with the abundance of strike-slip and oblique-slip slickenlines observed along this section of the Picuris-Pecos fault. Apatite in the metasedimentary rocks to the east of the

REFERENCES

- Bauer, P.W., and Kelson, K.I., 2004a, this volume, Cenozoic structural development of the Taos area, New Mexico: New Mexico Geological Society, 55th Field Conference, Guidebook, p. 129-146.
- Bauer, P.W. and Kelson, K.I., 1997, Geology of the Taos SW 7.5' quadrangle, Taos County, New Mexico: New Mexico Bureau of Mines and Mineral Resources, Open-file Geologic Map OF-GM 12, scale 1:24,000.
- Bauer, P.W., and Ralser, S., 1995, The Picuris-Pecos Fault – Repeatedly reactivated, from Proterozoic(?) to Neogene: New Mexico Geological Society, 46th Field Conference, Guidebook, p. 111-115.
- Bauer, P.W., Kelson, K.I., Heynekamp, M.R. and McCraw, D.J., 1999, Geology of the Ranchos de Taos 7.5-min quadrangle, Taos County, New Mexico: New Mexico Bureau of Mines and Mineral Resources, Open-file Geologic Map OF-GM 33, scale 1:12,000.
- Kelley, S.A., 1990, Late Mesozoic to Cenozoic cooling history of the Sangre de Cristo Mountains, Colorado and New Mexico: New Mexico Geological Society, 41st Field Conference, Guidebook, p. 123-132.
- Kelley, S.A., 1995, Evidence for post-Laramide displacement on the Picuris-Pecos Fault: New Mexico Geological Society, 46th Field Conference, Guidebook, p. 32-33.
- Kelley, S.A., Chapin, C.E., and Corrigan, J., 1992, Late Mesozoic to Cenozoic cooling histories of the flanks of the northern and central Rio Grande rift, Colorado and New Mexico: New Mexico Bureau of Mines and Mineral Resources, Bulletin 145, 39 p.
- McDonald, D., and Nielsen, K., 2004, Development of the Miranda graben constrains the uplift of the Picuris Mountains and has implications to the Rio Grande rift: New Mexico Geological Society, 55th Field Conference, Guidebook, p. 219-229.
- Miller, J.P., Montgomery, A., and Sutherland, P.K., 1963, Geology of part of the Sangre de Cristo Mountains, New Mexico, New Mexico Bureau of Mines and Mineral Resources, Memoir 11, 106 p.
- New Mexico Bureau of Geology and Mineral Resources, 2003, Geologic Map of New Mexico, 1:500,000.

beneath Arroyo Miranda, based on water-well records and the juxtaposition of Picuris Formation and granite. Good exposures in the Talpa/Llano Quemado area, where the Miranda fault zone cuts Picuris Formation, display numerous north-striking, strike-slip faults with map separations measured on the order of meters to hundreds of meters. Importantly, the <18 Ma middle Picuris Formation is cut by strike-slip faults within the Miranda and La Serna fault zones, suggesting that strike-slip faulting occurred during the Neogene, which is generally accepted to be dominated by rift extension.

Approximately 1 km east of the Miranda fault is a set of west-down branching fault splays (the McGaffey fault) located on the bedrock ridge of Cuchilla del Ojo. The McGaffey fault offsets Proterozoic and Paleozoic rocks, but appears to have considerably less throw than adjacent fault zones. Strike-slip slickenlines are common on north-striking, high-angle minor fault planes. Notably, the high-discharge Ponce de Leon warm springs are located at the intersection of the McGaffey and Embudo faults.

fault is rare and has a very low uranium content, resulting in the poorly constrained AFT age shown to the west of the fault on Figure 2.35.

In summary, AFT ages in the Talpa area do not record significant differential offset across the northern end of Picuris-Pecos fault system during early Laramide deformation in late Cretaceous to early Tertiary time. Instead, the AFT ages from the Pennsylvanian sandstones and the upper portion of the Proterozoic Miranda granite record slow regional Laramide cooling. Slow regional Laramide cooling is also observed in the Santa Fe Range to the south of the Peñasco embayment (Kelley, 1990; Kelley et al., 1992). Differential vertical motion associated with the transition between Laramide-aged transpression and Rio Grande rift extension seems to have occurred across some of the larger strands of the Picuris-Pecos system in this area, especially across the La Serna and Miranda faults, starting in late Eocene time. The timing of vertical motion across these faults is consistent with the timing of deposition of the Picuris Formation in the Miranda graben (Bauer and Kelson, 2004a, this volume).

The Rio Grande del Rancho fault zone, approximately 1.5 km east of the McGaffey fault, is a kilometer-wide complex family of west-down branching faults along, and east of, the Rio Grande del Rancho valley. Most of the main strand of the fault zone is buried in the alluvial valley, but excellent exposures in the valley walls show extensive strike-slip breccia/fracture zones in Pennsylvanian strata. At the northern end of the valley, Pennsylvanian bedding has been rotated into a vertical orientation along a west-down fault involving the Picuris Formation.

Return to vehicles and retrace route.

23.1 In the middle distance, at 12:00, is Blueberry Hill (Day 1, Stop 1), an erosional remnant of the middle Pleistocene Qf1 alluvial fan derived from the Rio Hondo and Rio Lucero drainages. The Qf1 fan deposits rest upon the pre-Rio Grande gorge Blueberry Hill deposits. The north-striking ridges and valleys west of Blueberry Hill are related to the Los Cor-

Table 2.2. Apatite fission-track data for Miranda graben area, Picuris Mountains

Sample Number	Rock Type	Latitude (N) Longitude (W)	Elevation (m)	Number of Grains Dated	rs x 10 ⁵ t/cm ²	ri x 10 ⁶ t/cm ²	rd x 10 ⁵ t/cm ²	Central Age (Ma) (±1 S.E.)	P(c)2 (%)	Uranium Content (ppm)	Mean Track Length (µm) (± 1 S.E.)	Standard Deviation Track Length
Picuris-Pecos fault at Telephone Canyon												
98SDC127	Proterozoic metasediment	36° 13.55' 105° 38.96'	2755	7	0.31 (9)	0.22 (31)	0.7893 (4567)	55.7 ± 21.0	97	3	-	-
98SDC128	Pennsylvanian arkose	36° 13.41' 105° 38.74'	2719	20	1.49 (122)	1.45 (592)	0.8016 (4567)	40.2 ± 4.3	<1	21	12.4 ± 1.4 (11)	2.3
La Serna fault traverse												
99SDC150	Proterozoic Miranda granite	36° 17.51' 105° 37.74'	2463	20	1.56 (95)	2.47 (752)	1.3957 (4607)	42.9 ± 5.0	95	21	13.6 ± 0.8 (24)	2.1
99SDC151	Proterozoic Miranda granite	36° 17.56' 105° 38.02'	2536	20	1.41 (158)	1.78 (997)	1.4095 (4607)	54.3 ± 5.2	68	15	12.6 ± 0.6 (76)	2.5
99SDC152	Proterozoic Miranda granite	36° 17.53' 105° 38.21'	2621	20	1.86 (125)	2.46 (826)	1.4275 (4607)	52.3 ± 5.4	99	20	12.7 ± 1.9 (5)	2.1
Cuchillo del Ojo												
98SDC133	Pennsylvanian sandstone	36° 19.14' 105° 34.93'	2164	6	1.3 (29)	1.1 (123)	1.128 (4607)	64.6 ± 13.4	98	11	-	-
99SDC149	Proterozoic Miranda granite	36° 19.25' 105° 36.38'	2249	20	1.11 (93)	2.18 (906)	1.3845 (4607)	34.6 ± 4.0	99	18	12.8 ± 0.6 (41)	1.9
East of fault system												
98SDC130	Pennsylvanian sandstone	36° 19.98' 105° 34.87'	2194	20	2.38 (267)	1.99 (1115)	0.8138 (4567)	47.4 ± 3.8	82	29	13.9 ± 0.9 (12)	1.6
99SDC153	Pennsylvanian arkose	36° 15.34' 105° 33.43'	2447	20	2.9 (344)	2.42 (1433)	1.1257 (4600)	65.6 ± 4.8	85	25	13.3 ± 0.5 (61)	1.8

rs - spontaneous track density

ri - induced track density (reported induced track density is twice the measured density)

Number in parenthesis is the number of tracks counted for ages and fluence calibration or number of track lengths measured.

rd - track density in muscovite detector covering CN-6 (1ppm); Reported value determined from interpolation of values for detectors covering standards at the top and bottom of the reactor packages (fluence gradient correction)

S.E. = standard error

P(c)2 = Chi-squared probability

ld = 1.551 X 10⁻¹⁰yr⁻¹, g=0.5

zeta = 4882.3 ± 307 for apatite

dovas faults (see Stop 1), a series of west-down normal faults that displace Servilleta Basalt on the east against Blueberry Hill deposits on the west. **0.4**

23.3 Ahead to the north is a fine view of the Taos Plateau volcanoes. We are driving north along the strike of the buried Picuris-Pecos fault system. Projected northward in the subsurface, these faults line up with the Questa section of the Sangre de Cristo fault system. The crescent-shaped valley from 12:00 to 2:00, the Taos embayment (Fig. 2.36), is a fault-

bounded section of the rift that is structurally younger than the last major movement on the Picuris-Pecos faults. The embayment is probably underlain by a shallow, structurally complex, bedrock bench. **0.2**

23.7 Turn left just past stop sign and start of paved road onto Camino Sur del Llano Quemado. **0.4**

24.3 Turn left heading northwest at paved intersection (unmarked). **0.6**



FIGURE 2.36. View northeast of the Taos embayment, an arcuate reentrant along the southern Sangre de Cristo Mountain front. The embayment may represent a late-rift structural domain that is separated from the older Taos graben by the buried, north-striking Picuris-Pecos fault system that includes the Miranda fault shown here (see Bauer and Kelson, 2004a, this volume for details).



FIGURE 2.37. View east along the Rio Pueblo de Taos of the 57,000-ton landslide that blocked NM-570 on February 3, 1993. The slide is developed in Pleistocene landslide deposits of Servilleta Basalt and interlayered sediment. The breakaway zone is well-defined, and visible in upper right corner of photo. Original road construction removed the toe of the naturally oversteepened slope, creating a wide zone of unstable material.

24.6 Turn left onto NM-68, and continue southward.

[40] 0.3

25.1 Taos County Road 110 (formerly NM-570) on the right is permanently closed about 5 miles west of here due to a small rockslide that blocked the road in 1992 (Fig. 2.37). This road still provides good access to the rim of the gorge and a view of the lower part of the Rio Pueblo de Taos valley where a steep knickpoint is developed on Servilleta Basalt. 0.5

26.5 Asymmetric drainages with relatively steeper eastern flanks are visible here and for several miles ahead (Fig 2.38). These drainages are developed in sand and gravel associated with the Qf1 and Qf2 alluvial fans sourced in the Picuris Range. 1.4

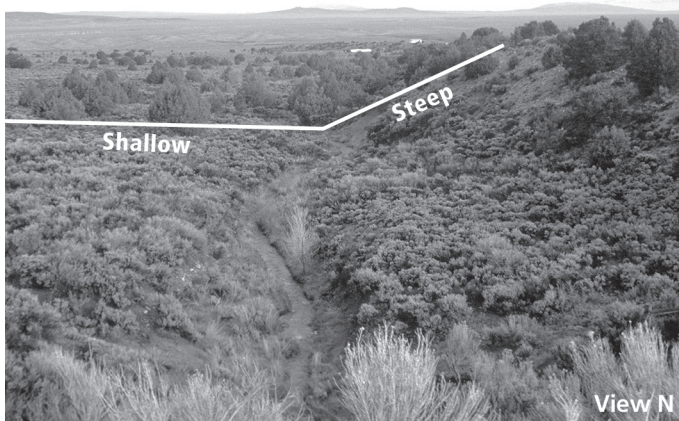


FIGURE 2.38. View west of one of many asymmetric arroyos developed on Quaternary alluvial fan deposits along the north flank of the Picuris Mountains. Along NM-68, the steep side is to the east, suggesting active east-tilting of this part of the basin.



FIGURE 2.39. Picuris Peak (10,801 ft), the highest point in the magnificent Picuris Mountains, provides one of the finest 360 degree panoramic views in the state--and, for your convenience, restroom facilities are available! The peak is underlain by a south-dipping strike ridge of ca. 1.7 Ga Paleoproterozoic Ortega Formation quartzite, one of the most erosionally resistant rock units in the Southwest.

27.6 Stakeout Drive on left. A white, somewhat reworked ash dated at 1.27 Ma by $^{40}\text{Ar}/^{39}\text{Ar}$ at New Mexico Tech (Bauer et al, 1999a) in Qf1 is correlated with the plinian phase of the upper Bandelier Tuff from the Jemez Mountains (N. Dunbar, personal commun., 1999). The reworked ash exposed in this roadcut is associated with the Qf1 fan surfaces shed from the Picuris Range, and provides age control for this unit and correlative terraces along the Rio Grande. The Qf1 fan and Qt1rg terraces overlie the uppermost Servilleta Basalt, and thus pre-date development of the Rio Grande gorge.

To the south, the Picuris Range rises to an elevation of 10,801 ft (3292 m) at Picuris Peak (Fig. 2.39). The Embudo fault extends along the northern flank of the range, and cuts the Qf1 and Qf2 alluvial fans. Scarps along the 1- to 2-km-wide fault zone are discontinuous, and there is geomorphic evidence of left-lateral deflection of several arroyos crossing fault strands. The fault zone extends through the remnants of a high, dissected alluvial-fan surface that is cut onto Tertiary sediments (Picuris Formation?) preserved along the Picuris Range front (Fig. 2.40). Local exposures of these rocks in arroyo walls near the range front show that individual fault strands typically are vertical. Muehlberger (1979) estimated that structural relief across the Embudo fault is at least 10,000 ft in this region, and the fault zone is dramatically displayed as a high-gradient lineament on the regional gravity map along the mountain front (Plate 3).

1.1

31.2 This Taos Valley overlook is OPTIONAL STOP 7 on [41] our return to Taos. This is one of the finest views in the state, and many first-time visitors to Taos stop here to gawk. 3.6

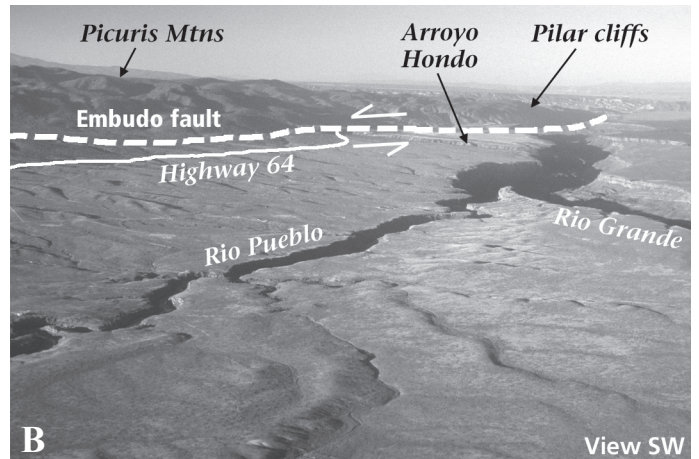
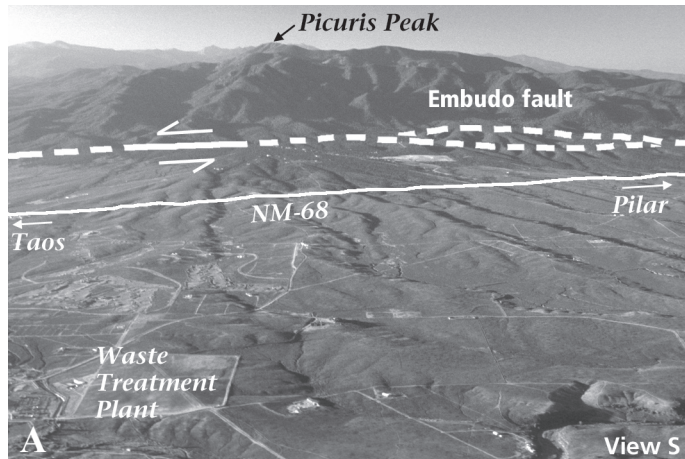


FIGURE 2.40. Oblique aerial photograph (A) looking south at the Picuris Mountains, the trace of the Embudo fault, and north-sloping alluvial fans on the piedmont of the Picuris Mountains. Oblique aerial photograph (B) looking southwest at the confluence of the Rio Pueblo de Taos and Rio Grande gorges, the Picuris Mountains, the trace of the Embudo fault, and the Pilar cliffs in the distance.

31.4 This curved section of NM-64 through Hondo Canyon (Fig. 2.41) is known locally as “the horseshoe bend” (for obvious reasons). Strands of the Embudo fault are clearly visible in the roadcut to the left. The outcrops along the horseshoe bend were made famous by Muehlberger (1979) in his original paper on the Embudo fault. Proterozoic rocks crop out a short distance up Hondo Canyon, including staurolite-bearing pelitic schists. Staurolites from the Rinconada Formation are commonly 90° interpenetration twins (‘fairy crosses’) and are mined and sold in local gem and mineral shops (Fig. 2.42). The arroyos that drain this section of the Picuris Mountains commonly contain gravels rich in garnets and staurolites. **0.2**

32.1 Mesa on the skyline at 12:00 is the basalt-capped Cerro Pedernal (the source of Pedernal chert). The low hill at 1:00 in the middle of the basin is Cerro Azul, a structural high composed of Proterozoic Ortega Formation quartzite that sits on a gravity high (Koning et al., 2004b, this volume) that may be related to the Tusas-Picuris fault of Karlstrom and Daniel



FIGURE 2.41. View north from the Picuris Mountains of the NM-68 horseshoe bend. The highway makes this dramatic bend southward because it must cross the deeply incised Arroyo Hondo, which drains the central Picuris Mountains and joins the Rio Grande in this photo.

(1993). The quartzite in Cerro Azul is identical to the Ortega Formation here in the Picuris Mountains and the Ortega Formation in the Tusas Mountains on the northwest skyline. **0.7**

32.7 The roadcut on the left exposes strands of the Embudo fault at the top of a long descent towards Pilar and the Rio Grande. Although this exposure contains a thin, conspicuous, south-dipping, strand of the fault, the main western strand of the Embudo fault across both these roadcuts is a 1-m-wide, near-vertical zone of fault gouge developed in the Tertiary sediments. Displacement on the south-dipping zone is relatively minor, and slickenlines on the fault plane suggest a sub-horizontal slip direction. The primary western strand of the Embudo fault zone in this area is a left-lateral fault, and the south-dipping secondary fault strand likely represents a positive flower structure within the fault zone. To the west, this western fault strand is located on top of Pilar Mesa, and then projects under the Rio Grande near Pilar.



FIGURE 2.42. Photograph of 4 cm wide, twinned staurolite, “fairy cross,” from the Hondo Canyon area, Picuris Mountains. This area is well known to northern New Mexico mineral collectors. New Mexico Bureau of Geology and Mineral Resources - Mineral Museum No. 12181

The Embudo fault in this area also includes a significant east-ern fault strand, located at the range front about 1 km southeast of this roadcut exposure. The eastern strand is near vertical based on its linear map pattern across substantial topography, and likely is the main fault strand from which the western fault branches. **0.6**

33.1 On the right are a series of roadcut exposures of the Ojo Caliente Sandstone (Fig. 2.43), of the Tesuque Formation of the Santa Fe Group. The Ojo Caliente Sandstone is a buff to white, well-sorted eolian sandstone, consisting mostly of fine sand. Tabular crossbeds are common, with some sets over 4 m in height. Transport was from southwest to northeast, at approximately 13-12 Ma (Steinpress, 1980). **0.4**

33.8 For the next several miles, NM-68 runs atop a major strand of the Embudo fault zone (Fig. 2.44) which has juxtaposed different members of the Tesuque Formation, and rotated bedding along the fault plane. The Rito Cieneguilla canyon on the left is underlain by structurally complex fault blocks of Tesuque Formation and Picuris Formation that are mantled by a sequence of Quaternary inset terraces (Kelson and Bauer, 1998). **0.7**

35.5 Steep gravel roadcut on left just before the Village of Pilar contains Proterozoic clasts from the Picuris Mountains, as well as placer staurolite and garnet. The major drainage on the left ahead is Agua Caliente Canyon, and contains the best exposure of the "Bradley conglomerate" of Leininger (1982). A white ash near the Bradley conglomerate has been dated at 34.5 Ma, suggesting that the conglomerate is a "pre-rift" deposit, probably equivalent to the lower lower con-



FIGURE 2.43. Although the Ojo Caliente Sandstone of the Tesuque Formation is best known for its beautifully preserved eolian dune forms, it also contains large round concretions in this area. These meter-wide concretions can be found in Rito Cieneguilla. Field book for scale.



FIGURE 2.44. Photograph of a steeply dipping, clay-rich fault zone in Tertiary sedimentary rocks of Rito Cieneguilla. This area is riddled by such Embudo fault zone structures, and makes estimates of stratigraphic thicknesses problematic.

glomerate member of the Picuris Formation (Bauer and Kelson, 2004a, this volume; Aby et al., 2004, this volume). **1.7**

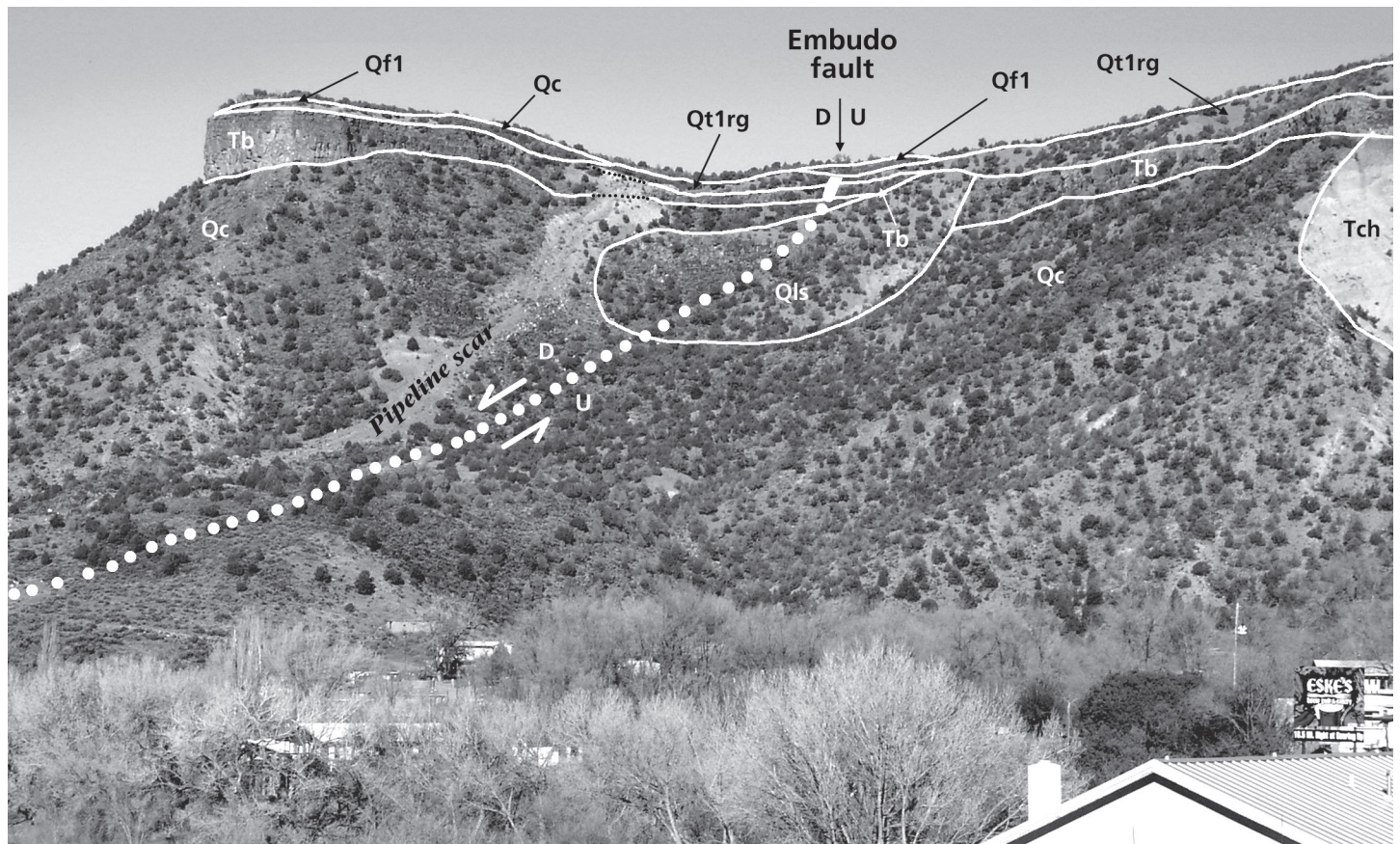
35.9 Village of Pilar. The Pilar Yacht Club is on the right. NM-96 on the right winds through this small arts colony to the BLM Orilla Verde Recreation Area which contains attractive day and overnight camping facilities along the Rio Grande. **0.4**

36.0 STOP 6. Rio Grande Gorge Visitors Center. [42] Turn left in the parking lot of the BLM

At this stop we will discuss the Proterozoic geology of the Picuris Mountains, the unusual mineralogy of the Pilar cliffs, rates of rift extension, the Embudo fault geometry and kinematics, Precambrian(?) versus Tertiary(?) diabase dikes, the Bradley conglomerate and the Picuris Formation, timing of uplift of the Picuris Mountains and age of the Embudo fault, new mapping on Pilar Mesa (Fig 2.45), and a reevaluation of the Chamita Member of the Tesuque Formation. **0.1**

Proterozoic geology of the Picuris Mountains:

The Picuris Mountains are composed of Proterozoic metasedimentary, metavolcanic, and metaplutonic rocks that range in age from about 1700 Ma to about 1440 Ma (Fig. 2.46). They are comparable to the rocks exposed in the Tusas Mountains to the northwest and the Truchas Peaks area to the southeast. All supracrustal rocks were repeatedly deformed and metamorphosed during Proterozoic time. The overall structure of the Picuris Mountains, best defined by the buckled and imbricated km-thick Ortega Formation quartzite, is that of a tight synclorium bounded by limb-parallel ductile shear zones. Folds are moderately inclined, horizontal, and are locally refolded, cleavage-transected, and cut by ductile faults. Three boundaries separate lithostratigraphic successions: (1) the south-dipping Pilar shear zone, which separates the Glenwoody Formation



55th NMGS FFC 2004
Second-day Road Log

FIGURE 2.45. Photograph looking northeast at the southern end of Pilar Mesa from STOP 6 at the BLM Visitor Center in Pilar. The Embudo fault exhibits about 3 m of northwest-down vertical separation of Servilleta Basalt (Tb) and ancestral Rio Grande gravel deposits (Qt1rg). Alluvial-fan deposits (Qf1) overlie the fault and are not displaced. Other labeled units are: Chamita Member of the Tesuque Formation (Tch), older alluvial-fan deposits (Qfo), landslide deposits (Qls), and colluvium (Qc).

from the overlying Hondo Group near here, shows both reverse and normal motion (Bauer, 1993); (2) the Plomo fault is a south-dipping, ductile reverse fault that separates the Hondo Group from the structurally overlying, but older, Vadito Group in the southern Picuris; and (3) the north-striking Picuris-Pecos fault, to the east that truncates both of the other boundaries, separates supracrustal rocks from an eastern plutonic terrane. Granitoids (1680-1450 Ma) intrude Vadito Group rocks only. The first two boundaries do not juxtapose different tectonometamorphic terranes, even though they are major shear zones. Strain heterogeneity appears to be characteristic of these rocks in this range and many of the Proterozoic-cored ranges of New Mexico. Folding and top-to-the-north shearing occurred during a progressive shortening event, perhaps related to the ca. 1650 Ma Mazatzal orogeny of Arizona and central New Mexico (Bauer, 1993).

Mineralogy of the Pilar cliffs area:

The Pilar cliffs (Figs. 2.47 and 2.48) contain a variety of unusual minerals. Although the steep and unstable slopes make collecting problematic, many of the minerals can be found in float along the base of the cliffs. The two most visually striking occurrences are found in the Mn- and rare-earth-element-enriched zone of the uppermost 30 m of the Glenwoody Formation. From the highway, the enriched zone is clearly

visible as a pink horizon below the massive gray Ortega Formation quartzite. The pink coloration is due to abundant pink muscovite (due to up to 6% ferric iron and traces of manganese) and the local appearance of piemontite, a deep red, prismatic,

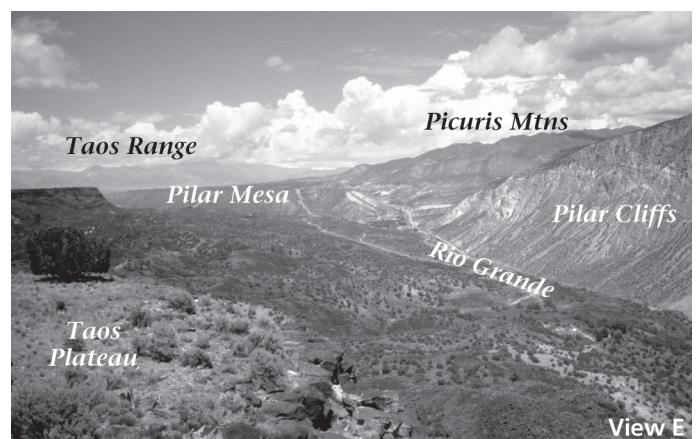


FIGURE 2.47. View east to the Village of Pilar showing some of the major physiographic features seen on Day 2. The Embudo fault zone lies at the base of the Pilar cliffs, and trends northeastward along the north flank of the Picuris Mountains. Pleistocene landslide deposits fill the Rio Grande gorge in the foreground, and Servilleta Basalt caps the Taos Plateau and Pilar Mesa.

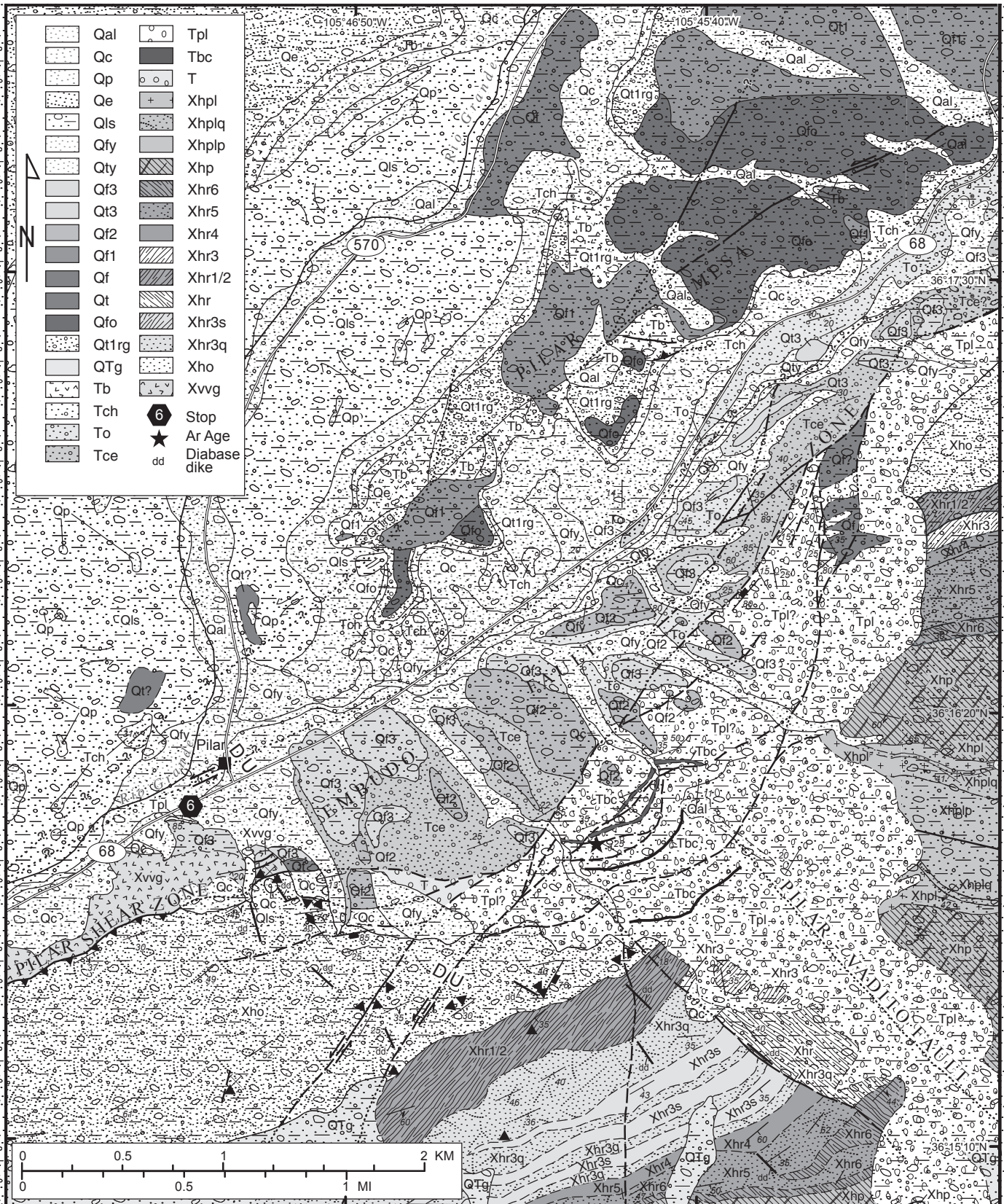


FIGURE 2.46. Geologic map of the Pilar area at STOP 6. This remarkable location displays a great variety of geologic features, including a Proterozoic ductile shear zone, uncommon and collectible minerals, a rift accommodation zone, an Eocene ash (35 Ma), pre-rift and rift-fill sediments, a sequence of Quaternary river terraces, and a major river. Modified from Kelson and Bauer (1998).

There's Gold in Them Cliffs...or is There? The Fleeting (and Fleecing?) Glen-Woody Mining Venture

Paul W. Bauer

New Mexico Bureau of Geology and Mineral Resources, New Mexico Tech, 801 Leroy Place, Socorro, New Mexico 87801

In the late 1890s, W.M. "Glen" Woody discovered gold in the Proterozoic metamorphic rocks of the Pilar cliffs, along the Rio Grande 5 km below the Village of Pilar. In 1902, Woody returned from the Klondike and began to develop his prospect with eastern venture capital under the auspices of the Glen-Woody Mining and Milling Company. Mr. Woody laid out a small town site on the north bank, named Glen-Woody, and built a bridge on the piers of an old government bridge that had burned in the 1870's.

Anticipating riches, the company constructed a flume that delivered Rio Grande water to power an impressive, 50-ton, experimental, cyanide mill on the south slope. The company began extracting ore from workings above the mill in what was alleged to be a huge low-grade gold deposit, principally in quartz.

Recent geologic mapping of the Pilar cliffs (Bauer and Helper, 1994; Kelson and Bauer, 1998) confirmed the existence of quartz veins in the Pilar cliff exposures of the Glenwoody Formation and overlying Ortega Formation. Such veins may indeed carry significant concentrations of gold (Schilling, 1960), and these units do crop out over a large area of the northwestern Picuris Mountains. However, the author is not aware of any published geochemical investigation of precious metal values in these rocks.

Although it was claimed that the ore ran \$1.40 to \$3.00/ton of gold, the best recovery by the mill was reportedly only \$0.40/ton. The body of gold ore was apparently of unacceptably low-grade and operating costs quickly exceeded income. The Glen-Woody venture proved spectacularly unsuccessful in a short period of time and operations were soon abandoned. The mill stood until at least 1917, as it appears in a photo with that date (Fig. 2.48). The town did not even exist long enough to get a post office.

Mr. Woody turned to operating a flour mill and a stage coach line, but the advent of the automobile doomed his operations, and the settlement bearing his name vanished. All that remains of the old mining operations are some timbers and scattered piles of mine waste and mill tailings on the slope above the road. The contemporary Glenwoody Bridge is actually located 200 m downstream of the original Glen-Woody Bridge.

Although little remains of this fascinating, short-lived mining venture, stock certificates occasionally appear on the market. One such collectible is an uncanceled, 8" x 10", stock certificate #556 of the Glen Woody Mining & Milling Co. (incorporated in New Mexico), that was issued to Mrs. Louise Rula Ross for 500 shares

in 1903. It was signed by president Wm. F. Frank and secretary R.C. Thomson. It contains a vignette of the mine and mill operations along the Rio Grande, and two smaller vignettes of miners working underground. The certificate has a green border and seal, and was printed by Goes.

As a postscript, the ill-fated Glen-Woody gold venture was not the last mineralogical dodge in the Pilar cliffs. Schilling (1960) reported that in the 1950s, some of the pink schist layers in the Glenwoody Formation were purported to contain lepidolite, an uncommon lithium-bearing mica, and valuable lithium ore. Although we now know that the primary pink minerals in the cliffs are pink muscovite and piemontite, due to the existence of the economically viable lepidolite-rich pegmatites in the nearby Harding Pegmatite Mine, a great deal of unwarranted interest was generated by the "discovery" of a huge lepidolite deposit in the Pilar cliffs. The Proterozoic rocks of the Pilar cliffs do contain a fascinating suite of unusual minerals, but lepidolite is not among them.



FIGURE 2.48. 1917 photograph of the mill site of the short-lived Glen-Woody Mining and Milling Company, established in 1902. This rare view of the wooden mill buildings was taken from the old mining camp, across the Rio Grande. Although the buildings and bridge are long gone, evidence of the operation can still be seen from the north slopes. Photo no. 32055 from the Adella Collier Collection, courtesy of the New Mexico State Records Center and Archives.

SOURCES

- Bauer, P. W., Love, J. C., Schilling, J. H., and Taggart, J. E., Jr., 1991, The Enchanted Circle-Loop Drives from Taos: New Mexico Bureau of Mines and Mineral Resources, Trips to the Geologic Past, no. 2, 137 p.
- Julyan, R., 1996, The place names of New Mexico: University of New Mexico Press, 385 p.
- Lindgren, W., Graton, L.C., and Gordon, C.H., 1910, The ore deposits of New Mexico: U.S. Geological Survey Professional Paper 68, 351 p.
- Schilling, J. H., 1960, Mineral Resources of Taos County, New Mexico: New Mexico Bureau of Mines and Mineral Resources, Bulletin 71, 124 p.

manganese epidote (Grambling, 1984). Below the contact with the Ortega Formation quartzite is a green, 2-ft-thick viridine-muscovite-quartz schist. Viridine is a bright-green variety of andalusite containing manganese and ferric iron (Grambling, 1984). Tourmaline (from Mg-rich dravite to Fe-rich schorl) is common throughout the Glenwoody Formation, and in the lowermost Ortega Formation (Modreski and Klein, 1999). A diverse suite of accessory minerals is associated with the tourmaline-rich zones, including fuchsite (Cr-bearing green muscovite), purple muscovite, epidote, clinozoisite, zoisite, thulite (pink zoisite), tremolite, sillimanite, kyanite, cyprine (blue idocrase), allanite, and stibiotantalite (Modreski and Klein, 1999).

Rates of rift extension from fault-offset Servilleta Basalt:

An estimate of slip for the last 3 Ma is based on the only known outcrop exposures of Servilleta Basalt south of the Rio Grande in the Picuris Range (Bauer and Helper, 1994). The small exposure is located in the Carson quadrangle on hill 7094' in T23N, R10E, S13. The base of the ca. 3 Ma basalt remnant is at approximately 7090 ft elevation, and its corresponding flow on the Taos Plateau is at about 6800 ft elevation. Assuming a 20° slickenline on a vertical Embudo fault, the minimum average net slip rate is approximately 100 m/m.y., with a minimum average vertical uplift rate of approximately 35 m/m.y. for the last 3 m.y. (Bauer and Kelson, 2004b, this volume). These slip rates can be used to estimate an average minimum east-west, net extension rate across the southern San Luis Basin of approximately 83 m/m.y. for the last 3 m.y. These estimates are generally consistent with earlier estimates of regional slip rates and extension rates in the northern Rio Grande rift (Bauer and Kelson, 2004b, this volume).

Embudo fault geometry and kinematics:

Machette et al. (1998) identified two sections of the Embudo fault based on a reversal of throw near the village of Embudo (Kelley, 1978; Personius and Machette, 1984). The 36-km-long northern section (the 'Pilar section' of Machette et al., 1998), was mapped in detail (Figs. 2.46 and 2.49) by Kelson et al. (1997), Bauer and Kelson (1997), and Kelson and Bauer (1998). The fault section extends from near the town of Embudo southwest of here, to an intersection with the Sangre de Cristo fault near the village of Talpa. A change in sense of vertical separation occurs over that section of the fault (see Kelson et al., 2004a, this volume). The northern Embudo fault is characterized by left-lateral slip (Muehlberger, 1978, 1979; Steinpress, 1980; Leininger, 1982; Hillman, 1986; Hall, 1988; Bradford, 1992; Kelson et al., 1997). Along the northern margin of the Picuris Mountains, the fault zone is as much as 2 km wide (Bauer and Kelson, 1997).

Ten kilometers to the southwest of this stop, the Embudo fault zone splits into two main strands (Koning et al., 2004b, this volume). The western strand, the La Mesita fault, has formed a prominent scarp on La Mesita and extends into the Velarde graben. The eastern strand is comprised of the Dixon and Velarde faults, which together with the Rio de Truchas fault form the eastern boundary of the Velarde graben. These two



FIGURE 2.49. A small exposure of Lower (?) Picuris Formation conglomerate is visible at the base of the slope behind the BLM Visitors Center at STOP 6. The steeply south-dipping strata attest to the proximity and scale of the Embudo fault. A lack of Picuris Mountains Proterozoic clasts and 25.1 Ma Amalia Tuff clasts suggests that these rocks are part of the pre-Embudo fault volcanoclastic apron that was shed off the San Juan volcanic highlands in Oligocene time.

strands (La Mesita and Dixon-Velarde faults) exhibit oblique slip movement (west-down, left-lateral). The Velarde and La Mesita faults terminate about 11-15 north of Española, and slip is interpreted to transfer westwards to an east-down, right(?) oblique-slip fault called the Hernandez fault (formerly called the Embudo fault; Aldrich (1986) and Aldrich and Dethier (1990)). The Hernandez fault has deformed the southern tip of Black Mesa and extends southwest to the Pajarito fault.

More recent mapping provides evidence of west-down fault displacement along the entire mesa. First, the east-facing scarp at the southern tip of the mesa is related to erosion by the ancestral Rio Grande. Unit Qt1rg is inset into the Servilleta Basalt, and there is no displacement of the basalt flow unit directly below the Qt1rg gravel. The ancestral Rio Grande, which flowed south across what is now the southern part of Pilar Mesa east of the present gorge, and incised into and removed several basalt flow units on the eastern side of the fault. This resulted in a prominent east-facing topographic scarp along the western margin of the ancestral Rio Grande channel during Qt1rg time.

Recent mapping also demonstrated the presence of west-down displacement of the Servilleta Basalt and overlying unit Qt1rg gravel at the southern end of Pilar Mesa (Kelson and Bauer, 1998). The base of unit Qt1rg displays about 3.5 m of net west-down displacement. Although there are several landslides at the southern end of the mesa that involve unit Qt1rg,

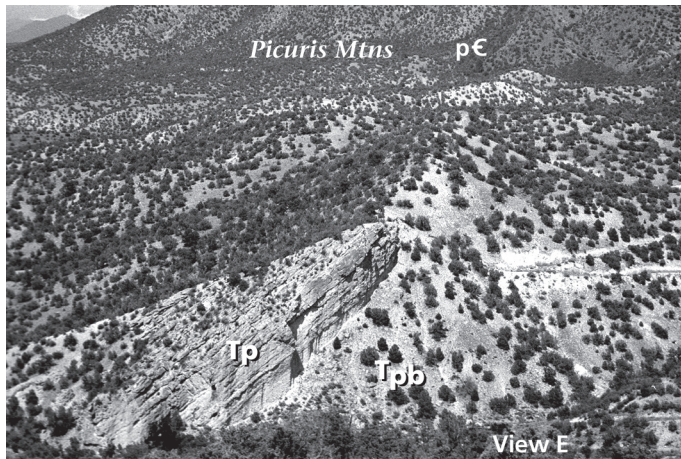


FIGURE 2.50. View east of the Rito Cieneguilla valley from the Picuris Mountains. The north-flowing drainage in the foreground is Agua Caliente Canyon, which contains the best exposures of the Bradley conglomerate of Leininger (1982). The lower half of the photo shows a north-dipping mesa of well-bedded, erosion-resistant Picuris Formation sandstone and conglomerate that overlies the “type section” of the Bradley conglomerate. The switchback road to the right exposes a deformed ash that yielded an $^{40}\text{Ar}/^{39}\text{Ar}$ age of ca. 35 Ma. The Bradley conglomerate is therefore interpreted to be a conglomerate layer within the Eocene/Oligocene lower member of the Picuris Formation.

Servilleta Basalt, and underlying Tesuque Formation, detailed mapping demonstrates that displacement is unrelated to landsliding. The lowermost flow unit of the Servilleta Basalt is continuous across the southern end of Pilar Mesa, with the exception of the 3.5 m west-down displacement at the Embudo fault.

Lastly, Muehlberger (1979), Leininger (1982), and Dungan et al. (1984) argue that the presence of one flow unit on the east side of the fault and multiple flow units on the western side is related to east-down displacement. These relations, and the continuity of the lowermost flow unit across the end of the mesa, are more easily explained by erosion of stratigraphically higher flow units by the ancestral Rio Grande. Incision of the ancestral river into the basalt removed the uppermost flow units, and the ancestral channel was filled with a thick (up to 30 m) section of Qt1rg gravel above the remaining lowermost flow unit. The Qt1rg gravel, in turn, is overlain by slate- and quartzite-rich alluvial-fan deposits derived from the Picuris Mountains (units Qfo and Qf1; Kelson and Bauer, 1998). This collection of field observations and interpretations of geomorphic history of Pilar Mesa lead to the conclusion that the Embudo fault, instead of having a reversal of vertical separation (a “hinge point”) on Pilar Mesa, is characterized by west-down displacement.

Bradley Conglomerate:

The Bradley conglomerate was first described and informally designated as the oldest member of the Tesuque Formation in the Pilar area by Leininger (1982). It is best exposed in Agua Caliente Canyon about 1 km south of NM-68 (Figs. 2.50, 2.51, and 2.52). The unit is mainly composed of well rounded, white to gray quartzite clasts that range in size from pebbles to boulders.

A minor clast constituent is pink granite, although clasts are up to 2 m in diameter. The conglomerate is very poorly sorted and unstratified, the matrix is predominantly coarse sand, and sedimentary structures are absent. Leininger (1982) estimated a poorly constrained maximum thickness of 650 m (2000 ft), and noted that it is unconformably overlain by the Chama-El Rito and Ojo Caliente members of the Tesuque Formation. He interpreted the unit as a debris flow that was derived from Ortega Formation quartzite and the Embudo granite in the Picuris Mountains to the south, and represents a syntectonic response of early-rift emergence of the Picuris Mountains at ca. 20 Ma.

Recent geologic mapping of the Carson quadrangle by Kelson and Bauer (1998) has added to our knowledge of this distinctive conglomerate. $^{40}\text{Ar}/^{39}\text{Ar}$ dating of 17 somewhat altered sanidine crystals from a white ash just southeast of the Bradley exposure yielded an age of 34.5 ± 1.2 Ma. They also mapped several similar quartzite-boulder conglomerate layers east of Agua Caliente Canyon, which appear to be interlayered with the lower Picuris Formation sandstones and siltstones. In addition, a number of subtle-but-significant bedding-parallel faults exist in the area. Furthermore, in the Talpa area to the



FIGURE 2.51. View of Bradley conglomerate exposed in Agua Caliente Canyon. Most of the clasts are well-rounded cobbles of Proterozoic Hondo Group quartzite.



FIGURE 2.52. The Bradley conglomerate contains rounded quartzite boulders that are up to a meter in diameter.

east, they mapped a similar quartzite conglomerate associated with Lower Picuris Formation that contains a 34.64 ± 0.16 white ash. They concluded that the Bradley conglomerate is part of a regionally extensive late Eocene to Oligocene Picuris Formation.

Reevaluating the Tesuque Fm and the Chamita Member:

The tilted exposures observed below the Servilleta Basalt on Pilar Mesa belong to the lower Cieneguilla member (Tesuque Formation) of Leininger (1982). There is an angular unconformity between these rocks and the coarser overlying upper Cieneguilla member. The coarsening-upward trend is attributed to higher rates of uplift of the Picuris Mountains in the latest Miocene-Pliocene (Leininger, 1982). Bauer et al. (1999a) have proposed subsuming the Cieneguilla member into the Chamita Formation of Galusha and Blick (1971). However, Koning (2003a) proposes abandoning the Chamita Formation for two reasons: 1. recent mapping by Koning and Manley (2003) and Koning and Aby (2003) indicate that strata associated with the Cejita Member and the informal piedmont facies of Manley (1976a, 1977, 1979a and b) east of the Rio Grande are also found in the Chamita Formation type section west of the Rio Grande. Ages interpreted from fossil assemblages (Tedford and Barghoorn, 1993) indicate that locally the Cejita Member and piedmont facies east of the Rio Grande are of the same

age as the lower Chamita section type section. 2. the base of the Chamita Formation is defined as unconformably overlying the Ojo Caliente Sandstone. However, the Ojo Caliente Sandstone does not extend significantly east of the Rio Grande. In the absence of the Ojo Caliente Sandstone, strata that are time-correlative to the Chamita Formation type section cannot be mapped. Thus, the Chamita Formation does not meet the mappability criteria mandated in the stratigraphic code for a formation-rank lithostratigraphic unit (The North American Commission on Stratigraphic Nomenclature, 1983). An additional complication is that locally the Ojo Caliente Sandstone extends into the late Miocene and interfingers with Chamita Formation strata.

Return to vehicles, exit parking lot, turn right on NM-64, and retrace route towards Taos.

40.3 Crossing Hondo Canyon. Dirt road on right leads into Carson National Forest land in the synclinal center of the Picuris Mountains. **4.3**

40.8 OPTIONAL STOP 7. Gorge overlook.

[41] Pull off into picnic area on right and park.

Photo opportunity and discussion of several prominent features of the southern San Luis Basin. **Be careful here as the view for drivers heading north is so suddenly arresting, that they often come to a screeching halt while hunting for their cameras.** This stunning view of the San Luis Basin (Fig 2.53) was recently protected by a historic multi-partner agreement that saved this land from development. The partners (BLM, Trust for Public Lands, New Mexico Congressional delegation, Taos Land Trust, San Felipe Pueblo, Santo Domingo Pueblo, and hundreds of New Mexico residents) formulated a multi-phased plan designed to allow the BLM to acquire the land. The property includes high mesa desert, cliffs of the gorge, and riparian areas along the Rio Grande. The property provides critical riparian habitat for peregrine falcon, native brown trout, and the federally listed endangered southwestern willow flycatcher. The BLM is currently developing a recreational and environmental plan for the property as part of the Orilla Verde Recreation Area. Looking north we see the widest part of the Rio Grande gorge where it is about the same size as the Hadley Rille at the Apollo 15 landing site on the Moon. This is why this area was used for exercises to simulate that lunar mission. Pictures of the exercise are in the separate articles by Muehlberger and Dickerson (2004, this volume). **0.5**

Embudo fault near Arroyo Hondo:

Based on exposures of reverse faults in Tesuque Formation roadcuts along NM-68 near here (Fig 2.54), Muehlberger (1979) postulated that the Embudo fault locally accommodates regional crustal shortening rather than differential crustal extension between rift basins. This interpretation led to the suggestion that the Española Basin, and the adjacent southern Sangre de Cristo Mountains between Taos and Santa Fe, have undergone counterclockwise rotation driven by oblique rift extension (Muehl-



FIGURE 2.53. Overview from Optional STOP 7 of the Rio Grande gorge and Pliocene volcanoes of the Taos Plateau volcanic field.

berger, 1979; Aldrich, 1986; Brown and Golombek, 1986). Thus, although the exposures of the Embudo fault in this area represent only a small glimpse of the structural character of the fault, they have played a critical role in the tectonic interpretation of the entire northern Rio Grande rift.

The 1.5-km-wide Embudo fault zone shows a complex pattern of deformation consisting of three major strands. The southern fault strand lies along the base of the Picuris Mountains front and is not exposed in any of the NM-68 roadcuts. This strand, which is associated with fault scarps developed on Qf1 fan deposits, likely continues southwestward into the Rito Cieneguilla valley, where it may be the primary strand of the Embudo fault zone.

The northern and middle strands cross NM-68 at roadcuts sketched by Muehlberger (1979), and merge into a single strand to the southwest. The northern fault strand has prominent geomorphic expression, with a prominent, 15-m-high north-facing scarp developed on Qf1 deposits (Machette and Personius, 1984; Personius and Machette, 1984), representing about 12 m of net north-down displacement of Qf1 deposits. As exposed in the NM-68 roadcut, the northern strand is a low-angle reverse fault along which sand and gravel of the Ojo Caliente Sandstone is placed over Qf1 deposits (Muehlberger, 1979). Qf1 deposits clearly are involved in multiple episodes of faulting, with at least one buried soil containing secondary calcium carbonate present on the downthrown side of the fault. Carbonate laminae on the north side of the fault are folded and faulted, and are involved in backthrusting near the ground surface. About 200 m east of NM-68, the northern strand of the Embudo fault is marked by a 1.5-m-high scarp across latest Pleistocene to Holocene fan deposits, and a left-deflection in a small arroyo (Kelson et al., 1997).

The middle fault strand exposed in the highway roadcut is associated with strongly tilted and folded Tertiary Santa Fe Group strata (Muehlberger, 1979). As sketched by Muehlberger (1979), the roadcut exposure shows a low-angle, north-vergent secondary thrust fault that dips about 30° southeast, and displaces beds within the Chama-El Rito Member of the Tesuque Formation. This secondary fault is dramatic but has less than 2 m of total stratigraphic separation. The amount of separation gradually decreases upward, with little or no discernible separation at the northern end of the roadcut (Muehlberger, 1979).

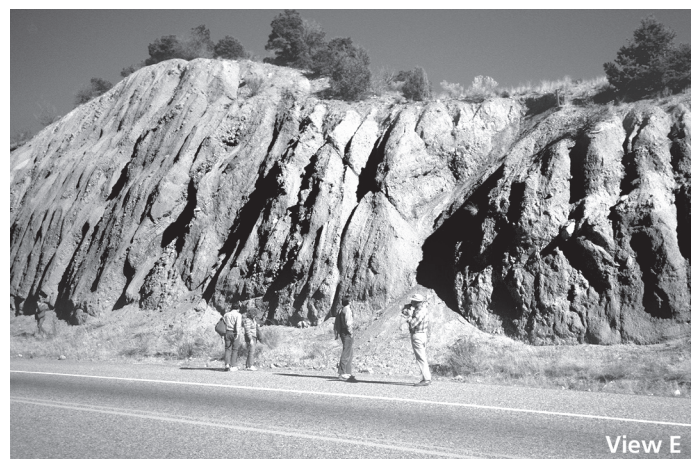


FIGURE 2.54. The outcrops of Tertiary sedimentary strata around the Horseshoe bend on NM-68 provided Bill Muehlberger and his students with the material for the first rigorous investigations of the Embudo fault, which Muehlberger insightfully described as an “intracontinental transform fault”. In this photo of Roadcut 2 (Muehlberger, 1979), Muehlberger (with bullhorn) narrates the history of these important exposures to a group of State Geologists in 1987.

The primary fault in the roadcut, which is located southeast of the secondary thrust fault, strikes 070°, dips moderately (50°) southeast, and juxtaposes sedimentary units within the Chama-El Rito Member.

The primary fault consists of a zone of shearing as much as 2 m wide that exhibits a minimum stratigraphic separation of 4 m of Chama-El Rito Member sediments. Kinematic indicators on the primary fault plane suggest left-lateral slip, including sigmoidal “s” shears in the fault zone and moderately plunging slickensides (15° toward S65°W, with a rake of less than 10°). On the western side of the highway, the roadcut exposes only a single, steeply northwest-dipping fault that juxtaposes distinct facies of the Santa Fe Group strata. This fault strikes 070, dips 82° northwest, and has grooves and mullions on the fault plane that plunge 20° to 23° southwest. These relations also suggest left-normal oblique slip along the primary strand of the Embudo fault. The prominent low-angle thrust exposed in the western roadcut likely is a minor reverse splay of the primary left-lateral fault strand, and perhaps indicates the presence of a local positive flower structure along the fault.

Thus, the northern section of the Embudo fault is a high-angle, oblique-slip fault with a component of northwest-side-down vertical separation. Thrust faults previously sketched by Muehlberger (1979) in NM-68 roadcuts splay upward from the trace of the high-angle fault and form a positive flower structure, and are secondary features that merge with a steep, left-oblique fault in the shallow subsurface. The primary strand of the Embudo fault is a steeply dipping to vertical structure that has had predominantly left-lateral slip. The northern fault strand is a secondary reverse splay that may be a result of a right step in the fault, which is consistent with interpretations of local shortening within restraining stepovers elsewhere along the fault (Steinpress, 1980; Hall, 1988).

Based on the local fault exposures near Arroyo Hondo, Muehlberger (1979) postulated that the Embudo fault locally accommodates regional crustal shortening. This led to the suggestion that the Española Basin, and the adjacent southern Sangre de Cristo Mountains between Taos and Santa Fe, have undergone counterclockwise rotation driven by oblique rift extension (Muehlberger, 1979; Aldrich, 1986; Brown and Golombek, 1986). This model interprets that movement on the Embudo fault involves north-vergent thrust faulting of the Picuris Mountains over the San Luis Basin. Thus, although the exposures of the Embudo fault in this area represent only a small glimpse of the structural character of the fault, they have played a critical role in the tectonic interpretation of the entire northern Rio Grande rift.

This previous tectonic model may be inappropriate on the basis of recent paleomagnetic data, regional fault activity assessments, and the re-interpretation of the horseshoe bend roadcuts. First, recent field studies by Salyards et al. (1994) provided data that argued against large-scale rotation of the Española Basin. Paleomagnetic data throughout the basin show non-uniform rotations, with greater amounts of rotation near basin-bounding faults (Salyards and Ni, 1990; Salyards et al., 1994). Second, active rotation of a structural block that includes the entire Espa-

ñola Basin and southern Sangre de Cristo Mountains requires similar rates and activities of the faults bounding this domain, including the Embudo, Pajarito, La Bajada, San Francisco, Tijeras, and Picuris-Pecos faults. However, regional assessments of fault activity (Wong et al., 1996; Machette et al., 1998) suggest that the activities and senses of slip along faults bordering the Española Basin and southern Sangre de Cristo Mountains are inconsistent with regional rotation. For example, the Pajarito fault along the western margin of the Española Basin is dominated by east-down normal displacement (Wong et al., 1996; Olig et al., 1996), the Picuris-Pecos fault shows no evidence of Quaternary activity (Machette et al., 1998), and there is an order of magnitude difference in the slip rates along faults along which the rotation should occur (Kelson and Olig, 1995). Lastly, recent mapping of the Embudo fault provides strong evidence of left-normal oblique slip and shows that the thrust faults in this area are secondary features related to a restraining stepover within a left-lateral fault zone. Thus, recent data do not support the hypothesis that the Embudo fault is associated with counterclockwise rotation of the Española Basin.

Why is the Rio Grande so straight?

The position of the Rio Grande and its gorge probably is related to the existence of the Gorge fault zone and the western edge of the Taos graben. Dungan et al. (1984) concluded that the position of the river is “controlled by a combination of overall east-tilting of the plateau, westward prograding alluvial fans, and the local control exerted by the faults, which in turn are surface manifestations of the deep Taos graben.” The gentle east tilt of the plateau likely forced the ancestral Rio Grande eastward, while the prograding fans probably constrained the amount of eastward migration. Possibly, the Rio Grande incised above the Gorge fault as a result of north-trending fracture zones in the basalts.

Return to vehicles, continue backtracking to Taos

42.7 Numerous piñon trees in this area were infected and killed by a fungus carried by bark beetles (see Mini-paper by McCraw). Because of long-term drought, trees in this area and throughout the Southwest are under stress. This stress has been compounded in many areas because, prior to overgrazing, grasslands once survived the range fires that kept trees from moving down slope. 1.9

49.4 Return to Sagebrush Inn. 6.7 [1] END OF DAY 2 LOG

Acknowledgments

We thank Taos Pueblo for permission to visit tribal lands. Brigitte Felix Kludt of Lemitar, NM, prepared many of the photos and figures. Sandra Azevedo and Kathy Glesener drafted the geologic maps and David McCraw made the trip-route figure.

An Overview of the Current Bark Beetle Infestation in New Mexico's Upland Forests.

David J. McCraw

New Mexico Bureau of Geology & Mineral Resources, Socorro, New Mexico 87801

In the first few years of the 21st Century, an unprecedented bark beetle infestation into the coniferous uplands of the American southwest has occurred, resulting in vast acreages of pine, spruce, and fir mortality. While these beetles are a natural component of forest ecology, widespread infestations have occurred here primarily in response to forest stress due to the onset of a prolonged drought in the region coupled with unnaturally over-thickened stands from a century of fire suppression. Under normal conditions, trees produce sufficient resins and have enough sap pressure to prevent beetle boring. However, in a stressed tree, individual beetles (which average 3-4 mm in size) can successfully bore through the bark and excavate a chamber where they release pheromones, calling mates and other beetles to the same tree. After mating occurs, the females excavate extensive tunnels into the cambium and lay egg galleries of 30-60 eggs in the lateral walls. In addition, many beetle species carry symbiotic microorganisms, which play an important role in killing the tree and nourishing the brood. After hatching, the larvae feed for 2-4 weeks on much of the remaining cambium, pupate, and transform into adults about 12 days after pupation, or roughly 40-55 days after the parents' initial attack (Kegley, *et al.*, 1997). The new adults bore back out of the now dead or dying individual, and seek out a new tree to continue the cycle. Normally, in New Mexico this cycle occurs 2-3 times per growing season. However, with the drier, warmer winters of 2001-3, beetles were often able to complete up to 5 life cycles per year (Swearingen, 2003), further exacerbating the infestation.

The highest rates of mortality in New Mexico have occurred in piñon (primarily *Pinus edulis* and *P. monosperma*) communities, with smaller areas of ponderosa pine (*P. ponderosa*) and Douglas fir (*Pseudotsuga menziesii*) affected. While there are numerous species of bark beetles in the region, the main culprits on piñon mortality here are the engraver beetles (*Ips spp.*, dominated by *Ips confusus*) while *Ips pini* and *Dendroctonus spp.* are attacking the ponderosa and fir. An initial outbreak of 13,000 acres of pine mortality was reported in 2000 for New Mexico after the first two years of severe drought (Cain, 2000). Prolonged drought intensified from the summer of 2001 to July of 2003, which statewide became the cumulative-driest month on record (NOAA, 2003). A statewide aerial survey ending in September 2003 (see Figure 2.55), documented a total area of pine mortality of 770,827 acres (Kim Paul, New Mexico State Forestry, personal communication). The majority of the affected area occurs on rocky, south-

west-facing slopes in the northern part of the state. It is generally believed that this infestation is far more widespread than the severe outbreaks that occurred during the 1950's drought, although historic records do not detail locations, extent, or severity. An accurate comparison is impossible because many of these historical records document overall forest mortality, including species of juniper (*Juniperus monosperma* and *J. deppeana*) and gambel oak (*Quercus gambelii*), which are generally not affected by bark beetles.

Although it is unclear how long the current drought and infestation will last, its effect on overall forest composition and ecology will endure well into the future. In the near term, loss of soil stabilization by tree roots coupled with an increased fire hazard in the coming years will result in significant erosion and topsoil loss. This degradation of habitat and loss of an important food source, piñon nuts, will likely have dire consequences for wildlife.

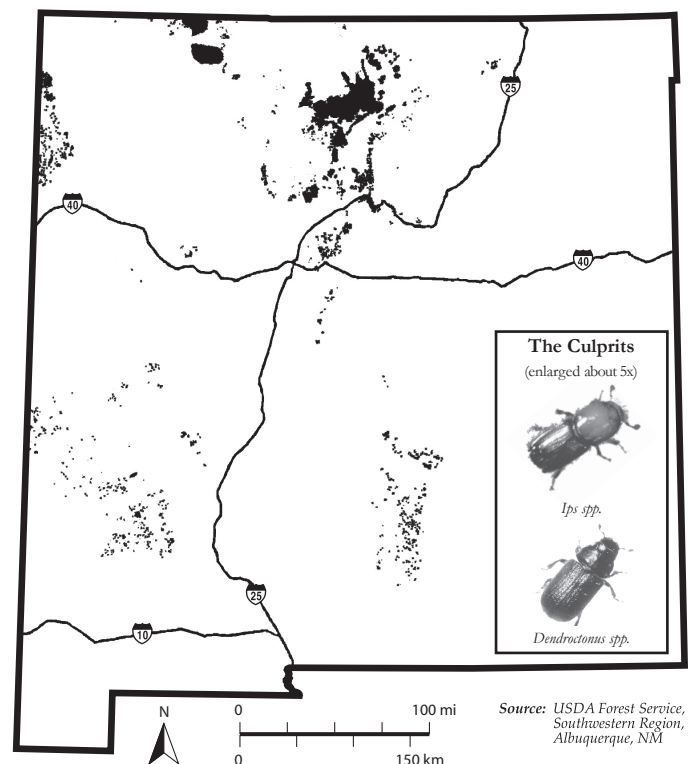
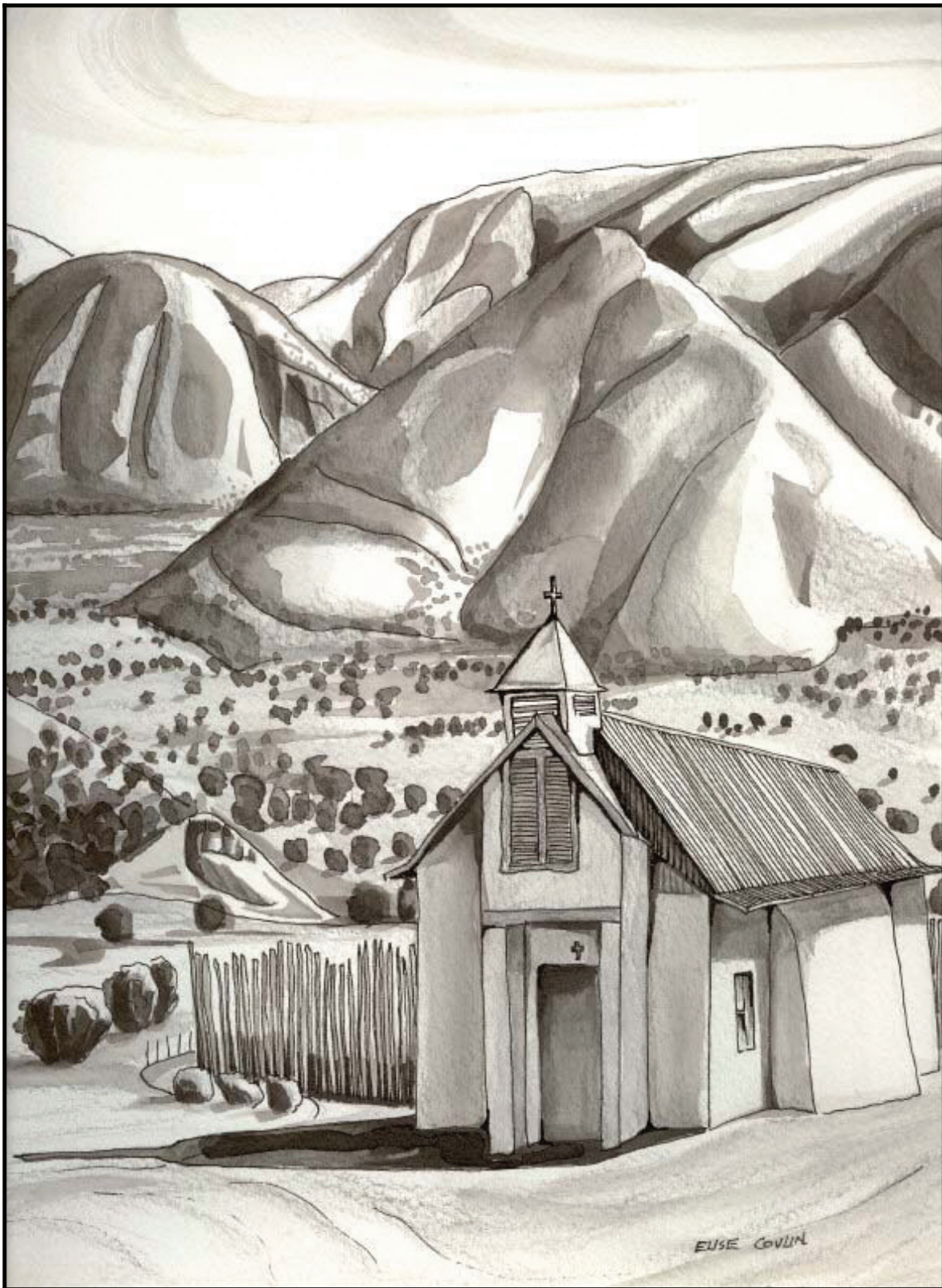


FIGURE 2.55. 2003 Mortality of piñon and ponderosa pine caused by bark beetles in New Mexico.

REFERENCES

- Cain, B., 2000, Drought increases bark beetle infestation throughout New Mexico: *New Mexico State University College of Agriculture and Home Economics News Archive*, Monday, November 2000, <http://www.cahe.nmsu.edu/news/2000/111300_beetles.html>.
- Kegley, S. J., Livingston, R. L., and Gibson, K., E. 1997, Pine engraver, *Ips pini* (Say), in the western United States: *USDA, Forest Service, Forest Insect and Disease Leaflet 122*.
- NOAA, 2003, *Climate of 2003 – July New Mexico drought*: National Climatic Data Center, 14 August 2003, <http://www.ncdc.noaa.gov/oa/climate/research/2003/jul/st029dv00pcp200307.html>
- Swearingen, K., 2003, Living with bark beetles in northern New Mexico: *The Taos Land Trust Newsletter*, No. 14, p. 1; 8.



Staurolite Hills of Pilar by Elise Covlin.

Courtesy of Brian and Julie Brister